Article

Neuron

Pbx Regulates Patterning of the Cerebral Cortex in Progenitors and Postmitotic Neurons

Highlights

- *Pbx1/2* function in progenitors and neurons patterns the prefrontal cortex
- *Pbx1/2* function in progenitors regulates D/V patterning
- *Pbx1/2* regulates cortical lamination of the frontal cortex through *Reelin* repression
- PBX directly regulates cortical promoters and enhancers

Authors

Olga Golonzhka, Alex Nord, Paul L.F. Tang, ..., Axel Visel, Licia Selleri, John L.R. Rubenstein

Correspondence

ogolonzhka@acetylon.com (O.G.), john.rubenstein@ucsf.edu (J.L.R.R.)

In Brief

Golonzhka et al. show that *Pbx1/2* transcription factors are required to generate the frontal cortex, in part by repressing dorsal cortical fate. *Pbx1/2* mutants have ventral expansion of *Reelin* expression, concomitant with inversion of cortical layering in the rostral cortex.

Accession Numbers

GSE73288

Golonzhka et al., 2015, Neuron *88*, 1192–1207
December 16, 2015
http://dx.doi.org/10.1016/j.neuron.2015.10.045

CellPress

CellPress

Neuron
Article

Pbx Regulates Patterning of the Cerebral Cortex in Progenitors and Postmitotic Neurons

Olga Golonzhka,[1,2,*] Alex Nord,[3] Paul L.F. Tang,[4] Susan Lindtner,[1] Athena R. Ypsilanti,[1] Elisabetta Ferretti,[8,9] Axel Visel,[5,6,7] Licia Selleri,[8] and John L.R. Rubenstein[1,*]

[1]Department of Psychiatry, Neuroscience Program and the Nina Ireland Laboratory of Developmental Neurobiology, University of California San Francisco, San Francisco, CA 94158, USA
[2]Acetylon Pharmaceuticals, 70 Fargo Street, Suite 205, Boston, MA 02210, USA
[3]Departments of Neurobiology, Physiology, and Behavior and Psychiatry and Behavioral Sciences, Center for Neuroscience, University of California Davis, Davis, CA 95618, USA
[4]Institute for Human Genetics, University of California San Francisco, 513 Parnassus Avenue, San Francisco, CA 94143, USA
[5]Genomics Division, MS 84-171, Lawrence Berkeley National Laboratory, Berkeley, CA 94720, USA
[6]U.S. Department of Energy Joint Genome Institute, Walnut Creek, CA 94598, USA
[7]School of Natural Sciences, University of California, Merced, Merced, CA 95343, USA
[8]Department of Cell and Developmental Biology, Weill Medical College of Cornell University, 1300 York Avenue, New York, NY 10021, USA
[9]The Danish Stem Cell Center, University of Copenhagen, Blegdamsvej 3B, DK-2200 Copenhagen, Denmark
*Correspondence: ogolonzhka@acetylon.com (O.G.), john.rubenstein@ucsf.edu (J.L.R.)
http://dx.doi.org/10.1016/j.neuron.2015.10.045

SUMMARY

We demonstrate using conditional mutagenesis that *Pbx1*, with and without *Pbx2*$^{+/-}$ sensitization, regulates regional identity and laminar patterning of the developing mouse neocortex in cortical progenitors (*Emx1-Cre*) and in newly generated neurons (*Nex1-Cre*). *Pbx1/2* mutants have three salient molecular phenotypes of cortical regional and laminar organization: hypoplasia of the frontal cortex, ventral expansion of the dorsomedial cortex, and ventral expansion of *Reelin* expression in the cortical plate of the frontal cortex, concomitant with an inversion of cortical layering in the rostral cortex. Molecular analyses, including PBX ChIP-seq, provide evidence that PBX promotes frontal cortex identity by repressing genes that promote dorsocaudal fate.

INTRODUCTION

Understanding the genetic underpinnings that control development of the frontal cortex is particularly important for understanding the evolution of complex computational modules found in higher mammals and for understanding mechanisms underlying neuropsychiatric disorders such as autism and schizophrenia. In these disorders, there is evidence for alterations in the size and function of the frontal cortex (Amaral et al., 2008; Crespo-Facorro et al., 2000; Gourion et al., 2004; Piven et al., 1995; Yamasue et al., 2004).

Regional patterning of the cerebral cortex is coordinately controlled by secreted factors such as fibroblast growth factor (FGF) 8, 15, and 17 and cell autonomously controlled by transcription factors (TFs), among other mechanisms. Loss of *Fgf8* and *Fgf17* expression leads to preferential deletion or hypoplasia of the frontal cortex (Cholfin and Rubenstein, 2007; Fukuchi-Shimogori and Grove, 2001; Garel et al., 2003). FGF signaling controls the gradiential expression of multiple TFs that contribute to cortical regional identity. For instance, the graded expression of TFs, such as *CoupTF1*, *Emx2*, *Lef1*, *Lhx2*, *Pax6*, and *Sp8*, along the rostrocaudal (R/C) and ventrodorsal (V/D) axes imparts regional identities to neuroepithelial cells in the ventricular zone (VZ) (Armentano et al., 2007; Bishop et al., 2000; Borello et al., 2014; Chou et al., 2009; Faedo et al., 2008; Galceran et al., 2000; Mallamaci and Stoykova, 2006; Mangale et al., 2008; Sahara et al., 2007; Yun et al., 2001).

Regional identity is then translated to the subventricular zone (SVZ) and cortical plate (CP). Initially, the CP also exhibits gradients of TFs (i.e., *CoupTF1* [*PD1*], *Bhlhb5*, *Lhx2*, *Tbr1*, and *Tbr2*) that are gradually converted to patterns with regional boundaries correlated with anatomical and functional subdivisions such as the frontal, motor, somatosensory, and visual cortex; there is evidence that these TFs also regulate regional fate (Alfano et al., 2014; Bedogni et al., 2010; Elsen et al., 2013; Greig et al., 2013; Joshi et al., 2008; Zembrzycki et al., 2015). At early developmental stages, thalamic afferents have little role in regional patterning (Miyashita-Lin et al., 1999; Nakagawa et al., 1999). Later in development, thalamic afferents contribute to refining cortical areal properties (Chou et al., 2013).

Here, we demonstrate that the *Pbx1* TF has a potent role in orchestrating the developmental elaboration of the mouse frontal cortex. We use a *Pbx1* conditional allele (Ficara et al., 2008) that was selectively deleted in the cortical VZ using *Emx1-Cre* (Gorski et al., 2002) or in newly generated cortical neurons using *Nex1-Cre* (Goebbels et al., 2006).

Pbx1 is one of four vertebrate *Pbx* genes; these are members of the TALE (three amino acid loop extension) homeodomain TF superfamily of atypical homeodomain-containing TFs, which include the invertebrate orthologs *exd* (*D. melanogaster*) and *ceh-20* (*C. elegans*) (Bürglin, 1997; Capellini et al., 2011b). These proteins have a PBC domain that promotes protein-protein interactions with two other TALE subclasses: MEIS and PREP (PKNOX). PBX/EXD proteins form complexes with HOX proteins, function

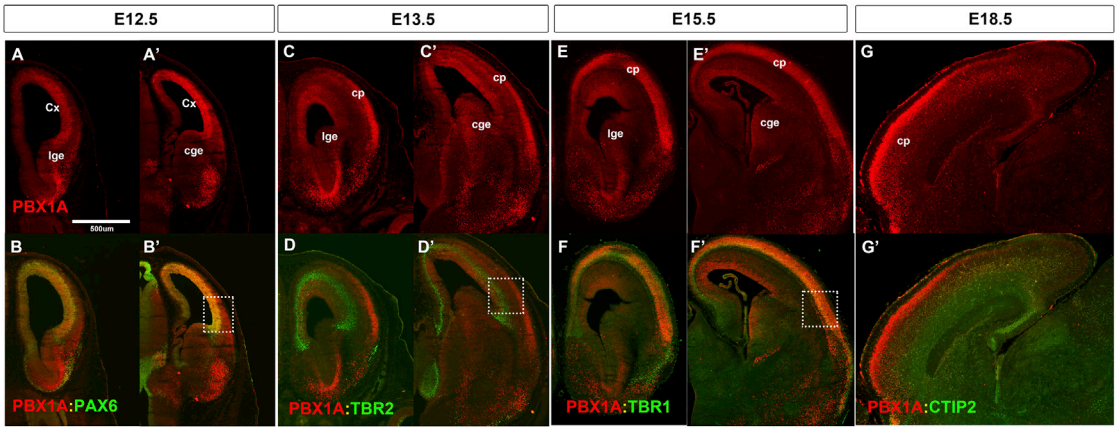

Figure 1. PBX1 Protein Is Expressed in Progenitors and Neurons of the Embryonic Cortex

Immunofluorescence co-staining at four prenatal ages with indicated antibodies.

(A–B′) PBX1A (in red) and PAX6 (in green) co-localize in the VZ of the cortex at E12.5 (coronal view).

(C–D′) PBX1A (in red) is expressed in the VZ and CP at E13.5. PBX1A and TBR2 (in green) do not co-localize in the SVZ of the cortex (coronal view).

(E–F′) PBX1A (in red) and TBR1 (in green) co-localize in the CP at E15.5 (coronal view).

(G and G′) PBX1A (in red) and CTIP2 (in green) is expressed at E18.5 (sagittal view).

Higher magnification and quantification of the images within the white rectangles are in Figure S1. Abbreviations are as follows: cp, cortical plate; Cx, cortex; cge, caudal ganglionic eminence; lge, lateral ganglionic eminence.

upstream of *Hox* genes, and control patterning of the anterior-posterior body axis and the limb bud (Capellini et al., 2011b; Vitobello et al., 2011). In addition, mouse *Pbx* genes have critical functions in regulating spleen, craniofacial, and skeletal development (Capellini et al., 2011a; Ferretti et al., 2011; Koss et al., 2012).

Pbx1–3 are expressed in the developing forebrain (Long et al., 2009; Toresson et al., 2000), but the function of these TFs has not been elucidated in these structures. Here, we found that loss of cortical *Pbx1* function alone, or in a *Pbx1;Pbx2*$^{+/-}$ sensitive background, led to hypoplasia and dyslamination of the frontal cortex through three mechanisms. In progenitors, *Pbx1* regulated R/C and dorsoventral (D/V) patterning. Surprisingly, abnormal D/V patterning resulted in ectopic *Reelin* expression in the rostral CP, leading to abnormal laminar patterning. In immature neurons, loss of Pbx1 resulted in loss of molecular features of the rostral cortex. Gene expression analyses identified dysregulated TFs (e.g., *Emx2* and *Lhx2*) that we propose contribute to abnormal cortical patterning through their functions in progenitors. We used PBX-chromatin immunoprecipitation sequencing (ChIP-seq) to identify genomic loci where PBX proteins bind in the embryonic day (E) 12.5 and E15.5 cortex. These results yielded evidence that PBX binds near *Emx2* and *Lhx2* promoters. Furthermore, we identified enhancer elements that are active in the E11.5 cortex that have PBX binding sites. Informatics approaches defined in vivo PBX binding sites, and provided evidence that these genomic elements also have signatures of combinatorial binding with other TFs.

RESULTS

Expression of *Pbx* RNA and Protein in Developing Mouse Cortex

We examined *Pbx1* RNA and protein expression in the developing cortex using in situ hybridization (ISH) and immunohistochemistry (IHC) with an antibody specific to the PBX1A splice variant of *Pbx1* (expression is lost in the *Pbx1* mutant) (Figures S1Q and S1R) (Phelan et al., 1995; Shen et al., 1996). PBX1A protein expression in the E12.5 cortical VZ showed a caudorostral gradient with low expression in the medial pallium (MP) and CP. Similar results were seen using RNA ISH (Figures S1A–S1F) (Allen Brain Developmental Atlas at E11.5, http://developingmouse.brain-map.org/).

PBX1A and PAX6 proteins were co-expressed in the cortical VZ (Figures 1A and 1B; Figures S1J and S1K), whereas PBX1a was not detected in secondary progenitors and was not co-expressed with *Tbr2* at E13.5 (Figures 1C and 1D; Figures S1L and S1M). By E15.5, PBX1a expression in the VZ was reduced, but it was extensive in the CP, where it was coincident with TBR1 in deep layers (Figures 1E and 1F; Figures S1N–S1P). At E18.5, PBX1A IHC labeled superficial layers of the CP, particularly in the rostral cortex (Figure 1G). *Pbx1* RNA expression closely matched protein expression (Figures S1A–S1F). Two other *Pbx* family members were expressed in the developing telencephalon. *Pbx2* was broadly expressed in progenitors at E12.5, E13.5, and E15.5 except for the MP (Figures S1G–S1I). *Pbx3* expression appeared largely restricted to the basal ganglia (http://developingmouse.brain-map.org/) (Toresson et al., 2000).

Cre-Mediated Elimination of *Pbx* Expression in Cortical Progenitors and Young Neurons

Pbx1 null mutants die because of hematopoietic defects in mid-gestation (DiMartino et al., 2001); therefore, we used *Pbx1* conditional mutants (*Pbx1*^{flox} allele) to analyze its function during cortical development (Ficara et al., 2008). To distinguish *Pbx1*'s role in progenitors versus neurons, we used two Cre lines: *Emx1-Cre* to delete *Pbx1* (*Pbx;Emx1-Cre*) in the VZ beginning at E10.5–E11 (Gorski et al., 2002) and *Nex-Cre* to remove Pbx1 (*Pbx;Nex-Cre*) in postmitotic neurons (Goebbels et al.,

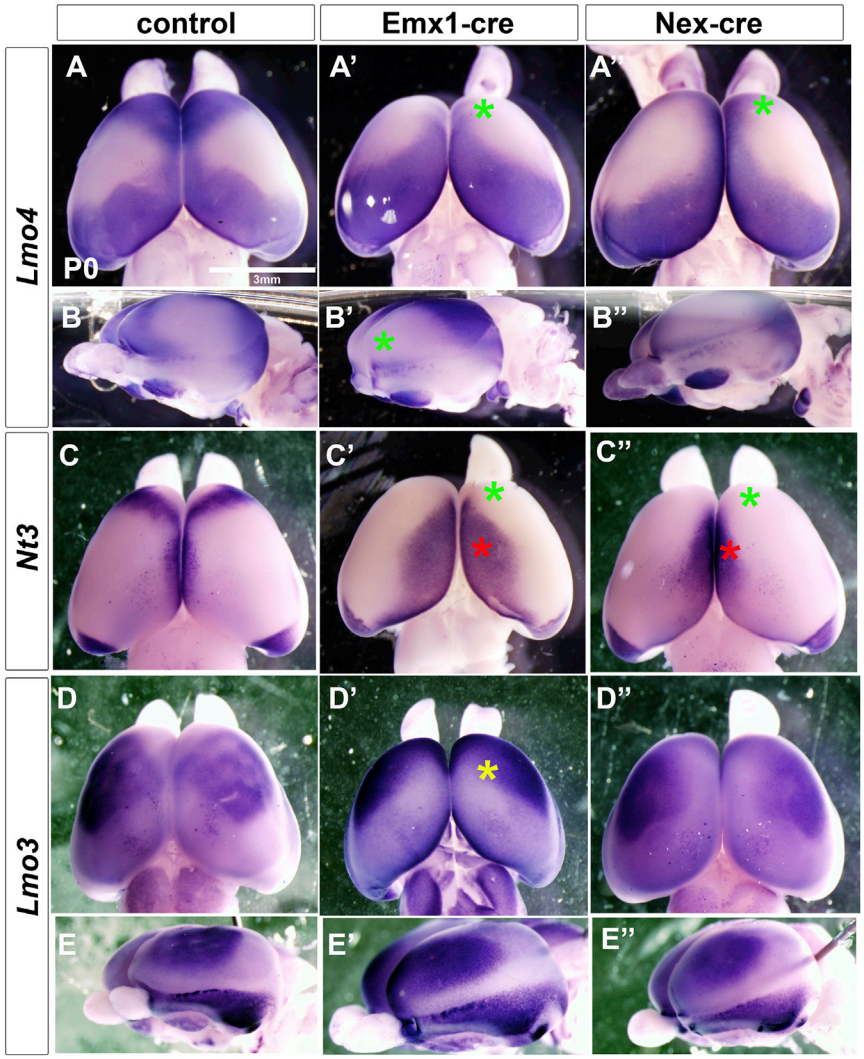

Figure 2. *Pbx* Mutants Have Major Alterations in Cortical Regional Patterning, Including Loss of Molecular Features of the Frontal Cortex

Analysis of the cortical patterning by WM-ISH on P0 brains of control (left column), *Pbx;Emx1-cre* mutants (middle column), and *Pbx;Nex-cre* mutants (right column).

(A–E) *Lmo4* probe: superior view (A–A″) and lateral view (B–B″). *Nt3* probe: superior view (C–C″). *Lmo3* probe: superior view (D–D″) and lateral view (E–E″). Green asterisks represent reduction of frontal cortex expression compared to control. Red asterisks represent expansion of dorsomedial cortical expression compared to control. The yellow asterisk represents a change in the frontal cortex expression pattern compared to control.

2006). Deletion was confirmed using *Pbx1* ISH (Figures S1Q and S1R). Although the *Pbx1* conditional mutants had cortical phenotypes (Figure S2H–S2K), we augmented the phenotype by reducing the *Pbx* dosage by including one *Pbx2* null allele (Figures S2I–S2O). Previous studies showed that the $Pbx2^{+/-}$ state exacerbated *Pbx1* non-brain phenotypes (Capellini et al., 2006), even though $Pbx2^{-/-}$ null mice were viable and had no obvious phenotype (Selleri et al., 2004). We observed an exacerbation of $Pbx1^{-/-}$ cortical molecular phenotypes in a $Pbx2^{+/-}$ background and therefore performed most of our analyses on the sensitized $Pbx2^{+/-}$ background. We did not observe a patterning phenotype in the $Pbx2^{+/-}$ mice (Figures S2F and S2G) and thus used $Pbx2^{+/-}$ as the control genotype. Our preliminary analysis suggests that the $Pbx2^{-/-}$ cortex is hypoplastic (data not shown).

Pbx;Emx1-Cre mutants were viable and survived into adulthood. The post-natal day (P) 7 *Pbx;Emx1-Cre* brain appeared grossly normal; histological analysis showed hypoplasia of telencephalic commissures, mild thinning of the caudal cortex, and dyslamination in hippocampal cornu ammonis fields (Figures S1T–S1Z). Herein, we focused on the phenotype of the prenatal cortex.

Pbx1 Regulates R/C Patterning in Both Progenitors and Postmitotic Neurons but Regulates D/V Patterning Primarily in Progenitors

Given PBX1 expression in the cortical VZ and its function in patterning of other tissues (Capellini et al., 2006; Selleri et al., 2001; Vitobello et al., 2011), we hypothesized that *Pbx1* may regulate cortical regionalization. Thus, we performed whole-mount in situ hybridization (WM-ISH) on P0 brains using *Lmo4*, *Nt3*, and *Lmo3* probes (Cholfin and Rubenstein, 2007, 2008). In control animals, *Lmo4* labels rostral (frontal) and caudal (visual) areas. *Pbx;Emx1-Cre* mutants lacked the $Lmo4^{+}$ frontal domain, and there was a rostral shift of the caudal *Lmo4* domain (Figures 2A, 2A′, 2B, and 2B′), providing evidence *Pbx1* regulates R/C cortical patterning.

To further assess the rostral phenotype, and to examine D/V patterning in the mutant, we studied *Nt3* (*Ntf3*) expression. At P0, in addition to labeling part of the frontal cortex, *Nt3* was expressed dorsally in the cingulate-retrosplenial cortex. Similar to the *Lmo4* phenotype, the *Pbx;Emx1-cre* mutant lacked the frontal *Nt3* domain and the dorsal domain expanded ventrally and rostrally (Figures 2C and 2C′). Finally, we examined *Lmo3* expression (a marker of the somatosensory cortex). The mutants showed a rostroventral expansion of this domain (Figures 2D, 2D′, 2E, and 2E′). Thus, *Pbx1* was required to promote rostral gene expression properties and repress dorsal ones in the developing cortex.

Because *Pbx1* is expressed in both cortical progenitors and neurons, we tested whether loss of *Pbx1* expression in postmitotic neurons regulated cortical patterning by studying *Pbx;Nex-cre* mutants at P0 using WM-ISH. These mutants lost frontal cortex expression of *Lmo4* and *Nt3* (Figure 2A″ and 2C″). However, the D/V patterning changes of *Lmo4* and *Nt3*

expression in *Pbx;Nex-cre* mutants were milder than those in the *Pbx;Emx1-cre* mutants (Figure 2).

We confirmed that the P0 WM-ISH expression changes led to the expected deletion of frontal cortex and expansion of dorsal and caudal cortex by performing ISH on P8 coronal sections of control, *Pbx;Emx1-cre*, and *Pbx;Nex-cre* brains (Figures S2P–S2GG″). For instance, in the frontal cortex, both mutants lost *Nt3* expression and had reduced *Cux2* and *Er81* expression, and the *Pbx;Emx1-cre* had greatly reduced *Lmo4* expression. The *Pbx;Emx1-cre* mutant also had ventral expansion of *Er81*, *Nt3*, and *Nurr1*. In all, the data provide evidence that *Pbx1* regulates RC patterning in both progenitors and postmitotic neurons but regulates D/V patterning primarily in progenitors.

Abnormal D/V Patterning in the *Pbx;Emx1-cre* Mutant Leads to Ectopic Reelin Expression in the Rostrodorsal Cortex, Leading to Dyslamination

As noted earlier, loss of *Pbx1* function led to ventral expansion of dorsal cortical properties (*Nt3* and *Lmo3*). In the rostral-most regions at E13.5 and E15.5, Reelin is expressed in a small domain adjacent to the septum, which is probably the indusium griseum (Figure 3).

In E13.5 *Pbx;Emx1-cre* mutants, this Reelin$^+$ domain broadly expanded ventrally in the CP (Figure 3A). By E15.5, a Reelin$^+$ deep layer in the CP extended ventrally from the dorsal-most position through roughly half of the cortex, but only in the rostral cortex, as seen in both coronal and sagittal views (Figures 3B–3E). These Reelin$^+$ cells did not co-express calretinin, and thus are probably not Cajal-Retzius neurons (Figures S3A–S3C).

Because Reelin regulates laminar positioning of cortical projection neurons (Ogawa et al., 1995), we assessed the expression of molecular markers of the subplate (*Nurr1*), layer VI (*Tle4*), layer V (*ER81*, *Etv1*), layer IV (*RORb*), and layer II/III (*Cux2*) at P8 (Hoerder-Suabedissen et al., 2009; Molyneaux et al., 2007; Nieto et al., 2004; Schaeren-Wiemers et al., 1997). Consistent with the ectopic *Reelin* expression in the deep CP, we observed an inversion of the cortical layers in the rostral cortex (i.e., the region with the ectopic *Reelin*) (Figure 4). Particularly note the inverted expression of *Nurr1* and *Tle4* in the superficial layers (cf. Figures 4A, 4A′, 4B, and 4B′), as well as *Cux2* and *RORb* inverted expression in the deep layers (cf. Figures 4D, 4D′, 4E, and 4E′). Bromodeoxyuridine (BrdU) birthdating analyses support the evidence for inverted lamination in the rostral cortex (Figure S4).

Pbx;Nex-cre mutants did not have the abnormal lamination phenotype (cf. Figures 4A–4E and 4A′–4E′). Thus, loss of *Pbx* function in progenitors, which lead to abnormal D/V patterning in the *Pbx;Emx1-cre* mutants, caused the ventral spread of *Reelin* expression into rostral deep cortical layers, with a subsequent inversion of cortical layers of the rostral cortex.

Molecular Mechanisms Underlying the D/V Patterning Defects in *Pbx* Mutant Cortical Progenitors: Altered TF Expression and Increased SMAD1/5 Phosphorylation

We next searched for the mechanisms through which *Pbx1* regulates patterning in cortical progenitors. FGF signaling regulates arealization and size of the frontal cortex, as exemplified by frontal cortex hypoplasia in *Fgf8* hypomorphs and *Fgf17* null mice (Cholfin and Rubenstein, 2007, 2008). Therefore, we examined the genetic interactions between FGF signaling and *Pbx1* function. First, we found that *Pbx1* expression appeared normal in *Fgf8*$^{neo/neo}$ hypomorphs, implying that *Pbx1* was not strongly regulated by FGF signaling (Figure S5J). Then, we examined expression of FGF-responsive genes (*Erm*, *Pea3*, and *Sp8*) in the VZ of the rostral cortex in E13.5 *Pbx;Emx1-cre* mutants. We detected no change in their expression, suggesting the *Pbx1* does not promote rostral identity by promoting FGF signaling (Figures S5A–S5C).

Like the *Pbx1* mutant, loss of *Pax6* function causes R/C and D/V patterning defects (Stoykova et al., 2000; Yun et al., 2001). However, *Pbx1* expression was not altered in *Pax6*$^{sey/sey}$ mutants at E11.5 and E12.5 (Figure S5K). Furthermore, *Pax6* expression was not altered in E13.5 *Pbx;Emx1-cre* mutants (Figure S2E). Together, these data suggest that *Pbx1* exerts its rostral patterning function independent of FGF signaling or *Pax6*.

We next turned our attention to *Pbx1*'s repression of dorsal properties, because upregulation of this system may alter frontal cortex development. We studied the expression of TFs that control cortical D/V patterning: *CoupTF1*, *Emx2*, *Lhx2*, and *Lmx1a* by ISH at E13.5 in *Pbx;Emx1-cre* mice. *CoupTF1* and *Lmx1a* had no clear expression changes (Figures S5D and S5H).

However, *Emx2* expression and *Lhx2* expression were increased, particularly in the ventral cortical VZ (red arrows) (Figures 5A–5D). *Lhx2* expression increased about 2-fold in mutant's ventral cortex and about 1.6-fold in the lateral cortex (Figure 5C). *Emx2* expression increased about 1.5-fold in the mutant's ventral cortex (Figure 5F). Both *Emx2* and *Lhx2* are critical in specifying cortical identities (Cholfin and Rubenstein, 2008; Chou et al., 2009; Mallamaci et al., 2000; Monuki et al., 2001; Muzio and Mallamaci, 2003). Thus, upregulation of *Emx2* and *Lhx2* could contribute to D/V and R/C patterning shifts in *Pbx1* mutants. *Lhx2* expression did not change in *Nex-cre* mutants (Figures S5S and S5T).

Next, to obtain unbiased information on *Pbx1*-regulated genes, we compared RNA expression (using gene expression array analysis) in the cortex from E12.5 and E15.5 control and *Pbx;Emx1-cre* brains. RNA expression changes were not strong at E12.5 (data not shown), whereas at E15.5 the *Pbx1* mutant had robust changes in RNA levels for several genes (Table 1).

We focused on TFs with altered expression levels (*Dbx1*, *Dmrta1*, and *Pknox1*) by performing ISH analysis. All three TFs were overexpressed in the cortical VZ (Figures 5G–5J and 6F′). *Pknox1* (also known as *PREP1*) is a co-factor of PBX1 (Berthelsen et al., 1998a, 1998b, 1998c). We performed overexpression experiments in which *Pknox1* was electroporated in utero at E12.5. However, this did not change *Lmo4* and *NT3* P0 WM-ISH expression (data not shown), suggesting that increased *Pknox1* did not contribute substantively to the *Pbx1* mutant phenotype but rather may reflect compensatory upregulation.

Dbx1 and *Dmrta1* expression were increased in the *Pbx;Emx1-cre* cortex; their expression domains expanded dorsally (Figures 5G–5J). *Dbx1* regulates D/V patterning of the spinal cord (Pierani

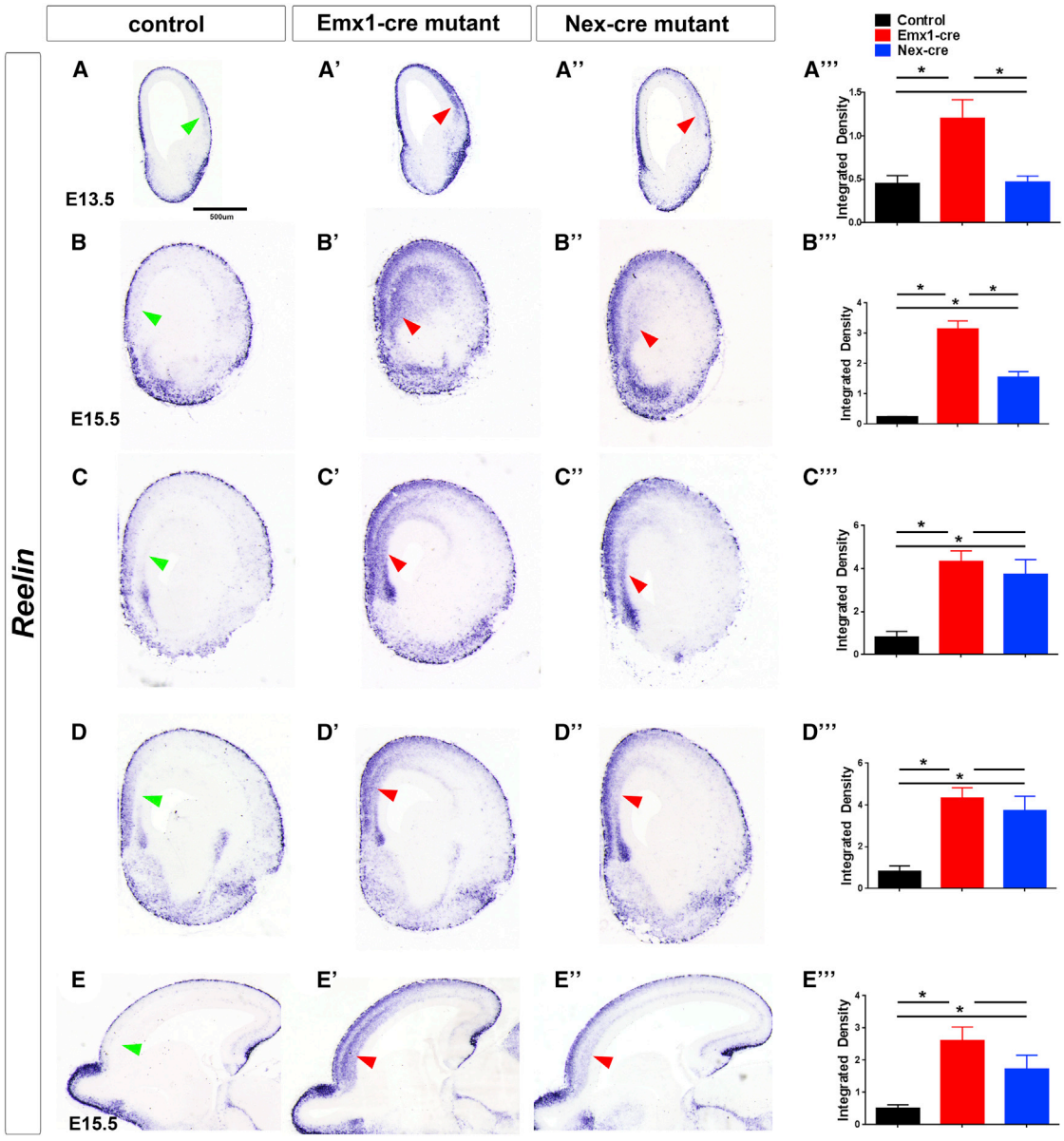

Figure 3. *Pbx* Mutants Have Ectopic *Reelin* Expression in the Rostral CP

Reelin RNA expression analysis by ISH in control (left column), *Pbx;Emx1-cre* mutants (middle column), and *Pbx;Nex-cre* mutants (right column).

(A–D) *Reelin* expression at E13.5 and E15.5 on coronal sections.

(E) *Reelin* expression at E15.5 on sagittal sections. Red arrows point to the increased *Reelin* expression in the mutant's rostral CP compared to the control (green arrows).

(A‴, B‴, C‴, D‴, and E‴) *Reelin* in situ signal intensity (integrated density) around the regions indicated by arrows was quantified and analyzed using ImageJ as described (McCloy et al., 2014). At least three brain sections were used for each measurement. *$p < 0.05$ (mean ± SD).

et al., 2001). *Dmrta1* loss of function analysis in the cortex has not been reported; however, its expression is increased by *Pax6*, implying that *Dmrta1* may promote ventral fate (Kikkawa et al., 2013). *Dmrta1*'s closely related family member *Dmrta2* regulates cortical DV patterning (Konno et al., 2012). Thus, we propose that *Pbx1* regulates D/V patterning, at least in part, by repressing TFs (*Dbx1*, *Dmrta1*, *Emx2*, and *Lhx2*) that are expressed in VZ cortical progenitors (in either D/V or V/D gradients).

In addition to molecular defects in the cortical VZ, *Pbx;Emx1-cre* mutants had dysregulation in the cortical SVZ. There was reduced expression of *Svet1* (~2-fold) and *Cxcl12* (~2-fold) (Figures S5M and S5N). The SVZ (but not the VZ) had an ~40% reduction of M-phase ($PH3^+$) cells at E12.5 in *Pbx;Emx1-Cre* mutants (not *Nex-cre* mutants) (Figures S5L, S5P, and S5Q). This could account for the reduction in the thickness of the superficial cortical layers. Furthermore, consistent with reduced *CXCl12*

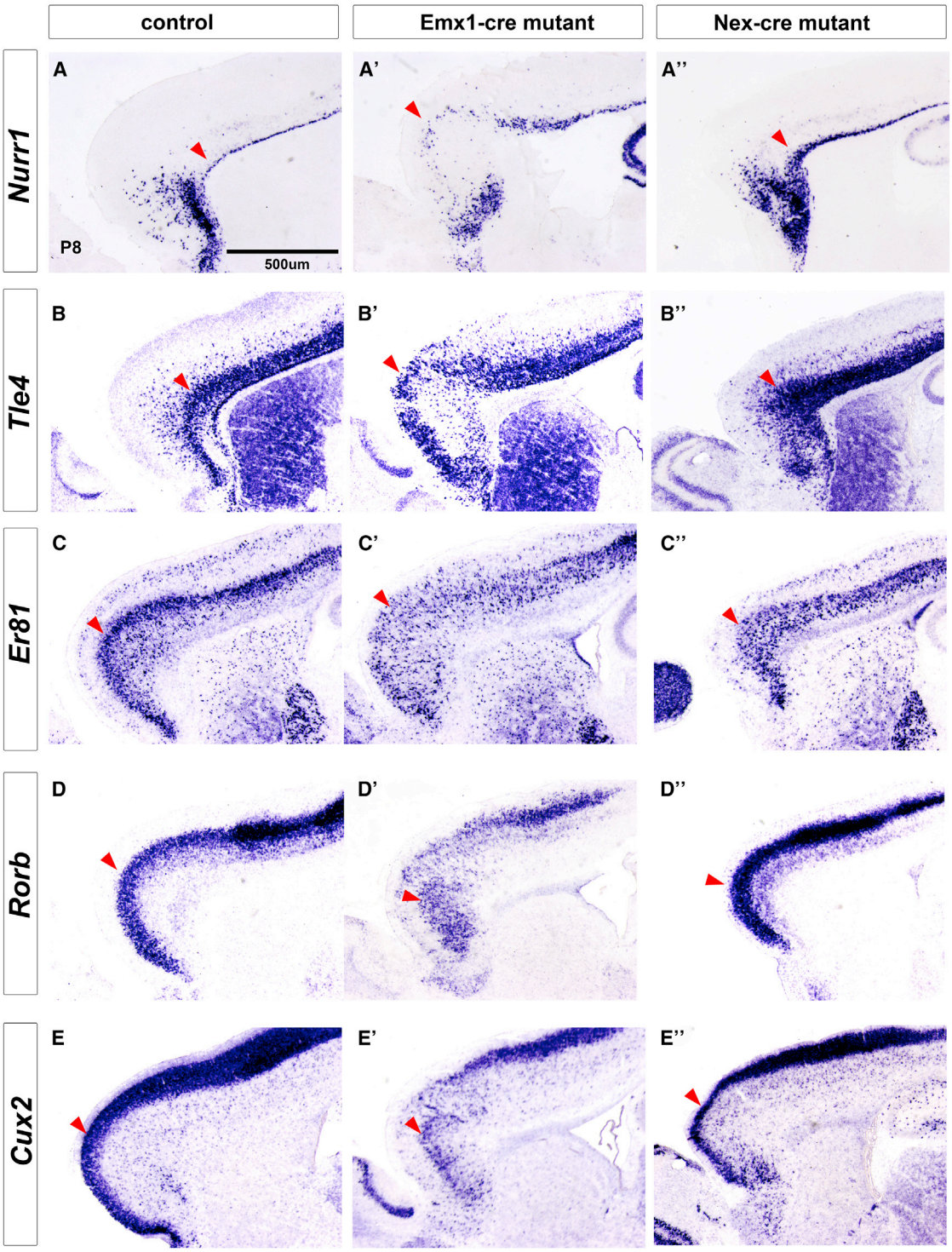

Figure 4. *Pbx* Mutants Have Inversion of Cortical Layers in the Rostral Cortex

Laminar marker expression in *Pbx;Emx1-cre* and *Pbx;Nex-cre* mutants at P8 by ISH on control (left column), *Pbx;Emx1-cre* mutants (middle column), and *Pbx;Nex-cre* mutants (right column).

(A–E) *Nurr1*, marker of subplate (A–A″); *Tle4*, marker of layer VI (B–B″); *Er81*, marker of layer V (C–C″); *Rorb*, marker of layer IV (D–D″); and *Cux2*, marker of layers II and III (E–E″). Red arrowheads point to the superficial boundary of the corresponding layers, showing the laminar inversions in the mutant.

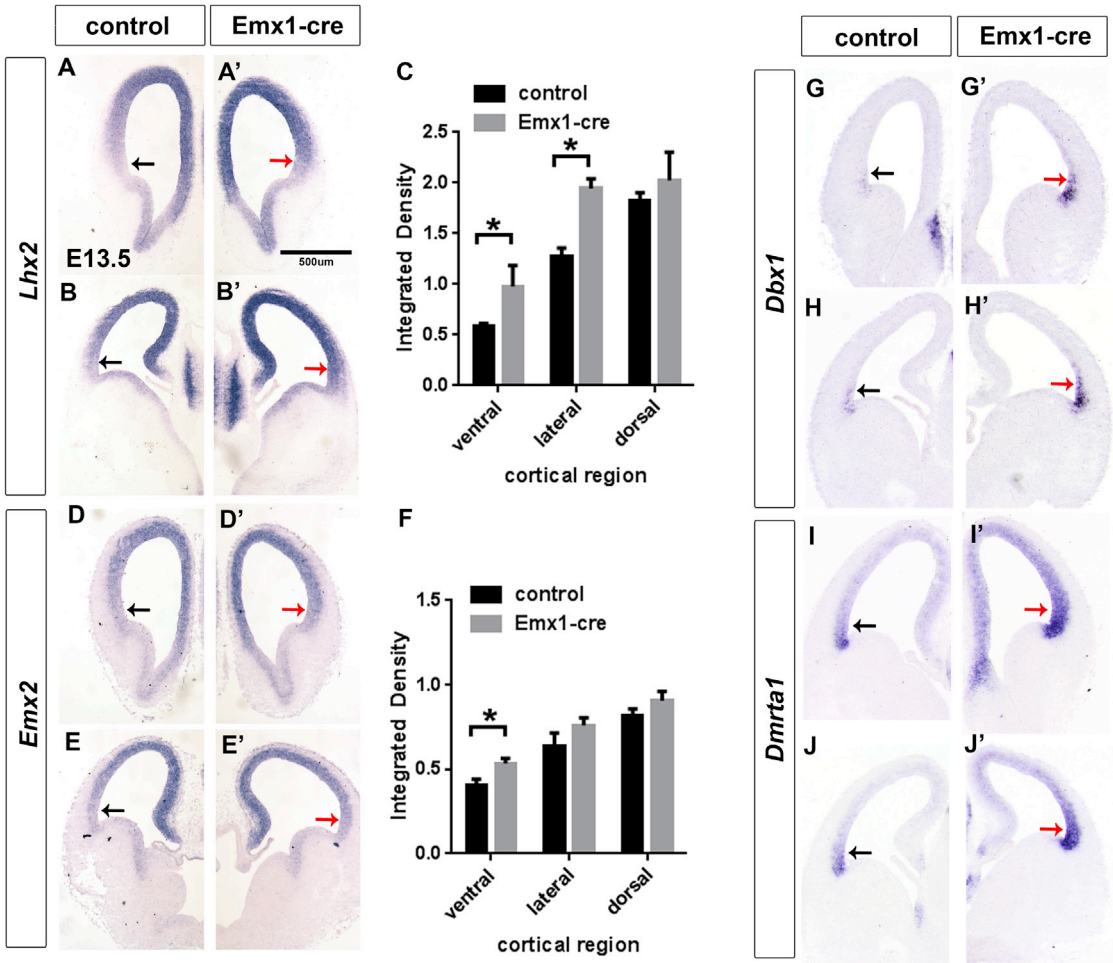

Figure 5. *Pbx;Emx1-cre* Mutants at E13.5 Have Changes in the VZ Expression of TFs that Control Cortical Patterning Shown on Coronal Sections Using ISH

(A and B, D and E, G–J) *Lhx2* expression (A–B′), *Emx2* expression (D–E′), *Dbx1* (G–H′), and *Dmrta1* (I–J′). Black arrows indicate normal expression in the ventrolateral cortex; red arrows point of the increase in expression of patterning genes in the mutant's ventrolateral cortex.

(C and F) Quantification of *Lhx2* (C) and *Emx2* (F) in situ signal in *Emx1-cre* mutant versus control cortex.

Measurements in four brain sections were made in the ventral, lateral, and dorsal regions of the cortex. Integrated density was calculated as described previously (McCloy et al., 2014). *$p < 0.05$ (mean ± SD).

expression, a known attractant for interneurons (Li et al., 2008; Wang et al., 2011), there were fewer *Dlx1*$^+$ and *Lhx6*$^+$ cells in the E15.5 *Pbx;Emx1-cre* cortex (data not shown).

Pbx repressed expression of *Cav1* (Figure S5O). *Cav1* is normally expressed at low levels in the dorsal-most cortex at E13.5; in the mutant, it is dramatically upregulated throughout the VZ. *Cav1* encodes a structural component of caveolae that plays an important role in integrating multiple signaling pathways.

Pbx was essential for the expression of *Smoc1* in the VZ of the cortex (Figure 6H′); ChIP-seq supports it as a PBX target (described later) (Figure 6H). *Smoc1* is an extracellular matrix protein that acts as a BMP antagonist in early embryogenesis (Thomas et al., 2009). As such, we tested whether BMP signaling may be abnormal in the *Pbx;Emx1-cre* mutants by measuring SMAD phosphorylation using IHC.

Phosphorylation of SMAD increases its ability to signal (Goumans and Mummery, 2000; Kitisin et al., 2007) and regulates DV patterning of the neural tube (Fernandes et al., 2007). pSMAD1/5 is normally detected in the VZ of the MP with a dorsal-to-ventral gradient at E15.5. *Pbx;Emx1-cre* mutants had increased pSMAD1/5 and a ventral spread along the VZ (Figures 6J and 6J′). This increase was detected throughout the RC extent of the cortex. pSMAD2 levels did not change (data not shown). pSMAD staining did not change in *Nex-cre* mutants (Figure S5V), and we did not observe a change in Bmp4 expression at E13.5 (Figure S5I).

WNT signaling is required for the dorsal-most cortical regions (Lee et al., 2000; Zhou et al., 2006), and it participates in neocortical patterning (Caronia-Brown et al., 2014) We assessed expression of *Axin2* and *Wnt3*, transcriptional readouts of WNT signaling. At E13.5, their expression appeared normal in

Table 1. Results of Gene Expression Array Analysis of the E15.5 *Pbx;Emx1-cre* Cortex, Showing Downregulated and Upregulated Genes

Genes Changed in Pbx1 Mutants			
Symbol	Name	Fold Change	FDR
Downregulated			
Smoc1[a]	SPARC related modular calcium binding 1	3.8	9.9×10^{-5}
Rai14[a]	retinoic acid induced 14	2.5	1.2×10^{-3}
Rbp1	retinol binding protein 1, cellular	2.4	4.5×10^{-2}
Flrt3[a]	fibronectin leucine rich transmembrane protein 3	2.3	1.8×10^{-2}
Ccbe1[a]	collagen and calcium binding epidermal growth factor domains 1	2.3	3.6×10^{-2}
Pdzrn3[a]	PDZ domain containing RING finger 3	2.2	1.1×10^{-3}
Bmpr1b[a]	bone morphogenetic protein receptor, type 1B	2.0	1.7×10^{-2}
Cxcl12	chemokine (C-X-C motif) ligand 12	2.0	5.5×10^{-3}
Cux2[a]	cut-like homeobox 2	2.0	3.8×10^{-2}
Fzd8	frizzled homolog 8	1.8	3.5×10^{-3}
Figf	c-fos induced growth factor	1.8	2.7×10^{-2}
Plxna4[a]	plexin A4	1.6	2.4×10^{-2}
Ngfr	nerve growth factor receptor	1.6	4.5×10^{-2}
Rnd2	Rho family guanosine triphosphatase 2	1.4	3.8×10^{-2}
Sema6d	semaphorin 6D	1.4	2.3×10^{-2}
Upregulated			
Dbx1	developing brain homeobox 1	4.6	9.0×10^{-3}
Pknox1[a]	Pbx/knotted 1 homeobox (Prep1)	3.0	9.9×10^{-5}
Npr3	natriuretic peptide receptor 3	2.8	1.4×10^{-2}
Pde1a[a]	phosphodiesterase 1A, calmodulin-dependent	2.3	2.7×10^{-2}
Dmrta1[a]	doublesex and mab-3 related TF-like family A1	2.3	3.3×10^{-2}
Fzd7	frizzled homolog 7	2.0	3.6×10^{-2}
Lmo3[a]	LIM domain only 3	1.9	3.1×10^{-3}
Lmo4[a]	LIM domain only 4	1.7	3.8×10^{-2}
Nr4a2 (Nurr1)	nuclear receptor subfamily 4, group A, member 2	1.7	2.3×10^{-2}
Ngef	neuronal guanine nucleotide exchange factor	1.6	2.7×10^{-2}

A red star indicates which genes have PBX ChIP-seq peaks in their promoter and/or intragenic regions.
[a]Genes that contain promoter or intragenic Pbx ChIP-seq peaks.

Pbx;Emx1-cre mutants (Figures S5F and S5G), providing evidence that *Pbx* does not mediate cortical patterning through modulating WNT signaling. Thus, abnormal regional patterning of the *Pbx;Emx1-cre* cortex appears to be due to alterations in the gradients of TF expression (*Dbx1*, *Dmrta1*, *Emx2*, and *Lhx2*) and increased SMAD1/5 signaling. We next assessed which of these phenotypes was directly due to *Pbx1* chromosomal binding.

PBX ChIP-Seq from Embryonic Cortex Identifies Target Genes

To determine which of the gene expression changes in the VZ may be directly PBX regulated, we performed ChIP-seq from E12.5 wild-type cortex using pan-PBX antibody. To help identify direct PBX targets in progenitors and postmitotic cells, we performed ChIP-seq from E15.5 cortex. As a specificity control, we added a PBX1 peptide to the chromatin immunoprecipitations to block antibody binding. About 4,100 peaks were identified at E12.5, and about 7,600 peaks were identified at E15.5. About 2,500 peaks were the same between E12.5 and E15.5. Genomic Regions Enrichment of Annotations Tool analysis (http://bejerano.stanford.edu/great/public/html/) (McLean et al., 2010) showed the distribution of PBX binding sites as a function of their distance from the transcription start site; ~35% were near the promoter (±5 kb), whereas the majority (65%) mapped at more distant locations at both E12.5 and E15.5 (Figures S6A and S6B).

We compared our E12.5 ChIP-seq peaks with 900 enhancers (Visel et al., 2013) that have reproducible tissue-specific enhancer activity in transgenic assays (Vista enhancer browser, http://enhancer.lbl.gov/). We found that about 30% of these 900 enhancers contained PBX peaks. Of enhancers that contained PBX peaks, about 40% had forebrain expression in the transgenic assay. Examples of four such enhancers are depicted in Figure S6C. These data support that PBX is frequently associated with bona fide distant-acting in vivo enhancers in general and with enhancers active in the developing forebrain in particular.

In addition, we compared a p300 ChIP-seq dataset from E11.5 forebrain (Visel et al., 2009) with our E12.5 ChIP-seq to evaluate how many PBX-enriched regions also map to p300-bound enhancers. Out of 2,453 p300-bound forebrain enhancers, 651 (26%) also contained Pbx ChIP-seq peaks.

Lhx2 and *Emx2* were upregulated in the ventral cortex of *Pbx* mutants (Figure 5). The promoter regions of these genes had PBX ChIP-seq peaks (Figures 6A and 6B). At E12.5 there were two prominent PBX ChIP-seq peaks at *Lhx2* promoters. PBX peaks were present in the same *Lhx2* genomic locations at E15.5 cortex, although they were not as pronounced. The *Emx2* locus contained two PBX peaks, one at the 5′ end and the other at the 3′ end of the gene (Figure 6B).

PBX had ChIP-seq peaks over the proximal promoters of *Pknox1* and *Meis2* genes (at E12.5 and E15.5) (Figures 6F and 6G). *Pknox1* and *Meis2* are members of the TALE homeodomain protein family that cooperatively bind with PBX proteins to promoters of target genes (Bjerke et al., 2011). In *Pbx* mutants, *Pknox1* expression is strongly increased throughout the cortex (Figure 6F′). Expression of Meis2 is also strongly increased in the VZ, as well as the CP, in *Pbx* mutants (Figure 6G′).

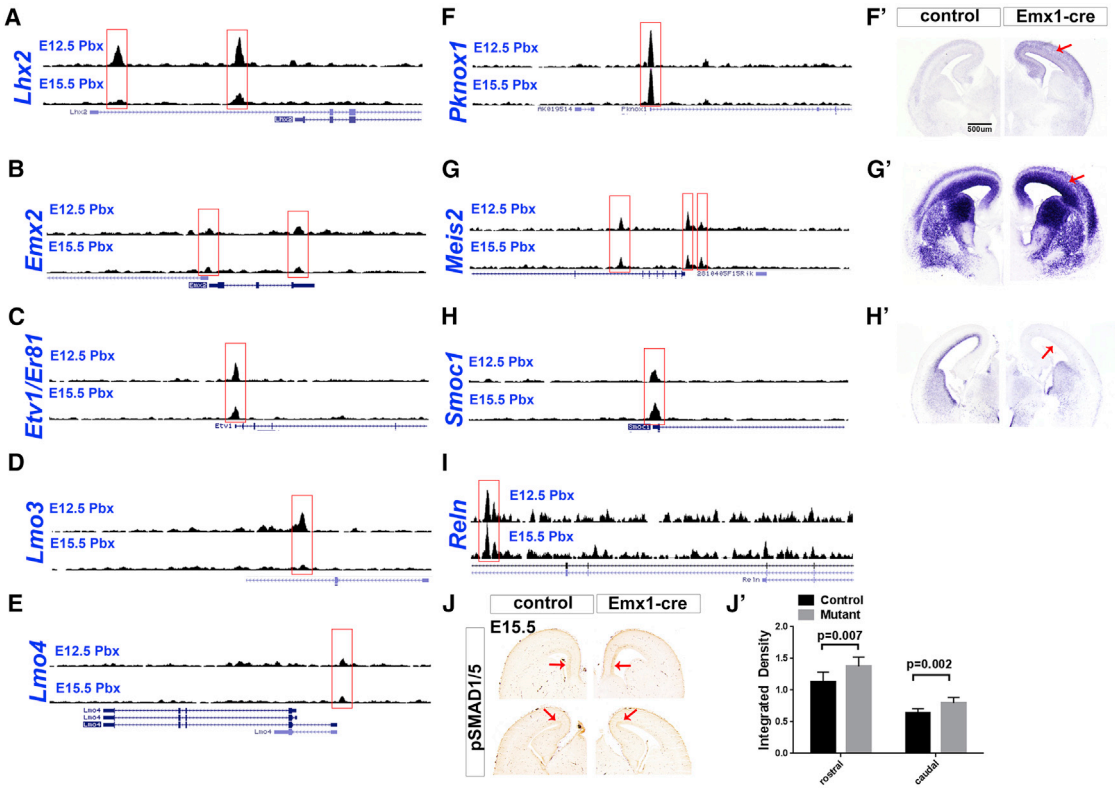

Figure 6. ChIP-Seq Showing PBX Binding to Promoters, and Other Gene Regions, that Are Dysregulated in *Pbx* Mutants

(A–I) Genome browser views showing PBX ChIP-seq peaks at E12.5 and E15.5. Gene expression changes are shown in Figures 2, 4, and 5, except for *Pknox1*, *Meis2*, and *Smoc1*, which are shown in (F)–(H′).

(J and J′) *Pbx;Emx1-cre* mutants have expanded domain of pSMAD1/5 expression in the dorsal cortex (red arrows) at E15.5. Signal intensity was quantified and expressed as integrated density in (J′) (mean ± SD).

PBX binding sites were also found in proximity of TFs that are preferentially expressed in specific cortical layers and regions. PBX ChIP-seq mapped to the start sites of *Etv1 (ER81)* (E12 and E15), *Lmo3* (E12), and *Lmo4*; expression of these three genes was dysregulated in *Pbx* mutant (Figure 4; Table 1; data not shown).

Although our analysis found many other interesting genes that are probable PBX targets, we wish to highlight *Reelin*. As shown in Figure 3, *Reelin* RNA expression was upregulated in the *Pbx;Emx1-cre* mutants (Figure 3). The *Reelin* locus contains two intragenic PBX peaks at E15 and one peak at E12 (which is in the same location as one of the E15 peaks) (Figure 6I).

Thus, there is good evidence that PBX binds to regulatory regions of genes whose abnormal expression is implicated in the regional and laminar phenotypes of *Pbx* mutants.

Nucleotide Motifs in Genomic Loci Bound by PBX

Next, we performed computational analyses to identify PBX in vivo binding sequences and to provide evidence for TFs that interact with the PBX-regulated genomic elements. We identified nucleotide sequences that were over-represented in the PBX-ChIP-seq peaks using the peak-motifs tool called Regulatory Sequence Analysis Tools (Thomas-Chollier et al., 2012) and clustered motifs by motif similarity and co-occurrence within ChIP-seq peaks using Pvclust (Suzuki and Shimodaira, 2006). Representative motif logos and frequencies for major identified motifs are shown in Figure 7 and Figures S7A–S7C. The most common motifs mapped to the MEIS1 motif in the JASPAR database, as well as PBX1 in JASPAR and in the Catalog of Inferred Sequence Binding Proteins database. The MEIS1/PBX1-annotated motif family included a long inverted palindromic motif and a short motif that represents half the palindrome (Figures 7A and 7B). We found that 77% of the identified PBX peaks at E12.5 and 79% of peaks at E15.5 contained at least one predicted motif, and these motifs showed strong enrichment at the center of PBX peaks, indicating that this is likely the primary binding motif recognized by PBX. The inverted palindrome motif and half-site have been identified previously using site-selection experiments with MEIS1 (Shen et al., 1997).

The most common secondary motif at both time points was a degenerate motif mapping to the SP/EGR families (53% of E12.5 peaks and 47% of E15.5 peaks) (Figures 7C and 7D). At E12.5, the second most frequent secondary motif was a strong PDX1 motif (36% of peaks). At E15.5, the second most frequent secondary motif was MECOM (46%), also correlated with the NFATC motif identified at E12.5. The co-occurrence of PBX1 and PDX1 has been previously reported (Swift et al., 1998).

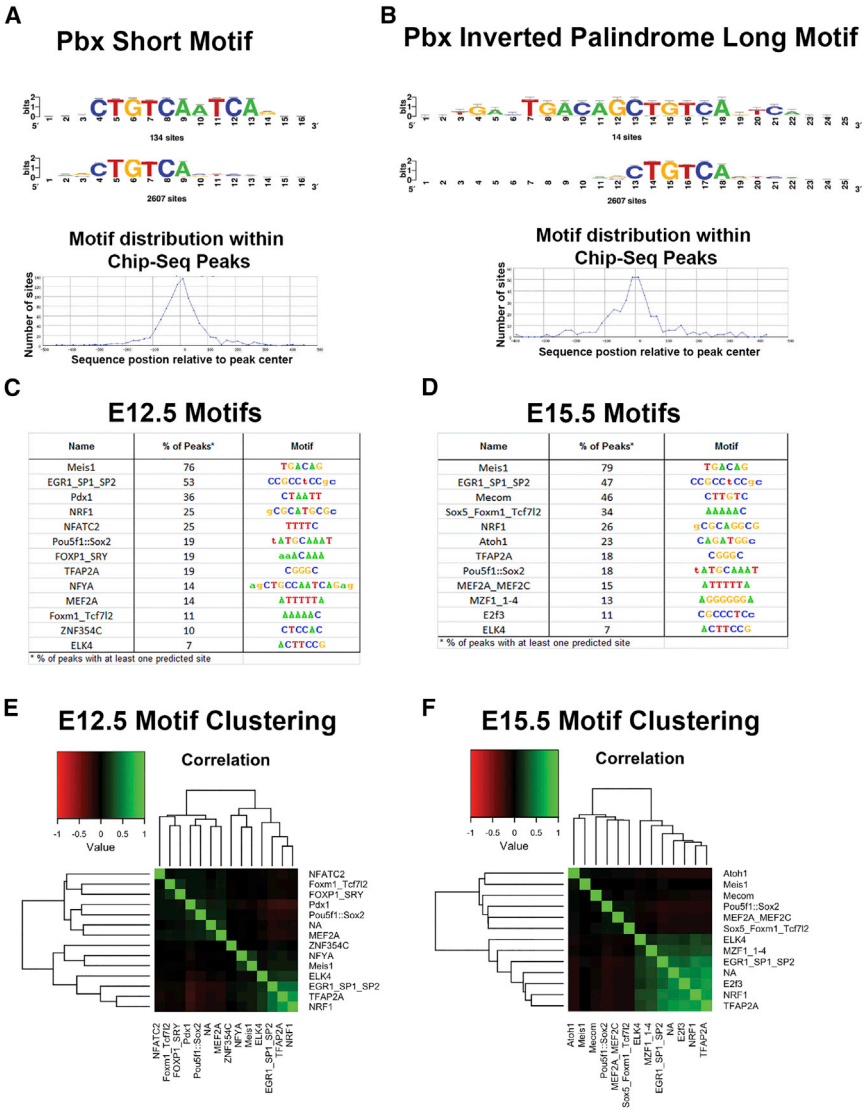

Figure 7. Motif Analysis of Genomic Loci Bound by PBX

(A and B) PBX short (A) and long (B) motifs identified from the ChIP-seq data. The long motif is an inverted palindrome. The sequence of both short and long motifs maps to the center of the PBX ChIP-seq peaks.

(C and D) Motifs identified in PBX ChIP-seq peaks at E12.5 (C) and E15.5 (D); their frequency is noted. The MEIS motif is the same as the PBX motif.

(E and F) Identification of TF motifs other than PBX/MEIS at E12.5 (E) and E15.5 (F).

We tested for differences in the distance to the nearest gene for identified motifs, revealing sets of motifs that are preferentially located proximal or distal to transcription factor start sites (TSSs). There was no difference for MEIS1 along with NFYA (highly correlated with MEIS1/PBX1 binding motifs and annotated to PBX1 in cisBP), FOXM1/TCF7L2, and ZNF354C. There was significant bias (t test, p value < 0.05) toward proximal PBX peaks for SP/EGR, NRF1, ELK4, MZF1_1-4, and TFAP2A motifs and bias toward distal PBX peaks for PDX1, POU5F1::SOX2, NFATC2/MECOM, FOXP1/SRY, MEF2A, ATOH1, and SOX5. Clustering of motif co-occurrence captures the strong enrichment for TSS-proximal motifs, with little minimal structure observed for motifs preferentially found distal to the TSS at both time points (Figures 7E and 7F; Figures S7D and S7E).

Finally, we tested for motifs that were enriched at one time point but not the other using peak motifs with the background as the second time point. At E12.5, PDX1/NOBOX motifs are strongly enriched compared to peaks identified at E15.5, with 64% of E12.5 peaks annotated with this site. SP/EGR family motifs are also enriched relative to E15.5. At E15.5, we identified ATOH1, NFIC/HAND1::TCFE2a, and FOXD3, all three of which were preferentially located distal to TSSs. ATOH motifs were found in nearly 70% of E15.5 PBX peaks when analyzed with E12.5 as the background. The increased frequency of occurrence for NOBOX/PBX1 at E12.5 and ATOH1 at E15.5 is at least partly driven by these motifs clustering with MEIS1 sites in the original analysis using the peak-motif default background.

DISCUSSION

Herein, we demonstrate using conditional mutagenesis that *Pbx1* regulates regional identity and laminar patterning of the developing mouse neocortex in cortical progenitors (using *Emx1-Cre*) and in newly generated neurons (using *Nex1-Cre*). Because *Pbx1* and *Pbx2* have similar RNA expression patterns at E11.5 (Figure S1), and because they are known to share functions (Capellini et al., 2006), we amplified the cortical phenotype by eliminating one *Pbx2* allele. Analyses of *Pbx1* mutants with normal *Pbx2* dosage were qualitatively the same as the compound mutant (Figure S1). Furthermore, cortical patterning appeared normal in $Pbx2^{+/-}$ (Figure S2).

We found three salient molecular phenotypes of cortical regional and laminar organization: (1) hypoplasia of the frontal cortex in both *Pbx;Emx1-Cre* and *Pbx;Nex1-Cre* (Figure 2; Figure S2), (2) ventral expansion of the dorsomedial cortex in *Pbx;Emx1-Cre* (Figure 2), and (3) robust ventral expansion of *Reelin* expression in the CP of the frontal cortex, concomitant with a partial inversion of cortical layering in *Pbx;Emx1-Cre* (Figures 3 and 4). The latter is a novel phenotype in which abnormal cortical patterning is coupled with region-specific abnormal laminar patterning. Next, we address mechanistic underpinnings of these phenotypes.

Pbx Function in Cortical Progenitors Regulates D/V Patterning by Repressing *Lhx2* and *Emx2* Expression

We propose the *Pbx* regulates cortical regional fate in the cortical VZ in part by repressing expression of TFs that control cortical DV patterning. *Pbx;Emx1-cre* mutants have ventral expansion of high *Emx2* and *Lhx2* expression. The mutants also exhibit dorsal expansion of *Dbx1* and *Dmrta1* (from the ventral-most cortex) (Figure 5). Concomitant with these changes in the VZ are a dorsal-to-ventral expansion of molecular properties in the CP that is particularly striking for *NT3* (Figure 2; Figure S2). There is no clear ventral-to-dorsal expansion of CP properties. We propose that the loss of frontal cortex properties (loss of *Lmo4* and *NT3* and gain of *Lmo3*) is in part due to the rostroventral shift of caudodorsal properties (e.g., Lmo3) (Figure 2).

The changes in expression of *Lhx2* and *Emx2* could contribute to the *Pbx* mutant's patterning phenotype, because each of these TFs has demonstrated functions in cortical patterning. *Lhx2* promotes neocortical fate by repressing properties of flanking structures. *Lhx2* null mutants illustrate that *Lhx2* dorsally represses choroid plexus identity and that ventrally *Lhx2* represses properties of the ventral pallium (also known as antihem) (Bulchand et al., 2001; Mangale et al., 2008; Monuki et al., 2001). In *Lhx2*;*Emx1-cre* mutants, lateroventral cortex acquires neocortical fate (Chou et al., 2009). Thus, like *Lhx2*, *Pbx* controls the balance of cortical fates along the DV axis. In *Pbx* mutants, the *Lhx2* gradient is changed; there is upregulation in the lateroventral regions of the cortical VZ and in the CP. Dorsal properties are expanded (e.g., $NT3^{+}$ cingulate or retrosplenial) at the expense of more ventral properties ($Lmo3^{+}$ somatosensory). Thus, we propose that *Pbx* maintains the correct level of *Lhx2* expression, which is crucial in regulating the balance among different cortical regions.

Emx2 overexpression is also likely to contribute to the *Pbx* mutant phenotype. An ~2-fold increase in *Emx2* expression in the VZ repressed rostroventral fate and led to expansion of caudodorsal cortical areas (Hamasaki et al., 2004). As noted earlier, this phenotype is similar to that of the *Pbx* mutant. ChIP-seq analysis identified two PBX peaks just 5′ of the transcribed region of *Lhx2* and two PBX peaks within *Emx2*'s transcribed domain (Figure 6). Thus, PBX may directly control *Lhx2* and *Emx2* transcription.

Molecular Mechanisms Underlying the D/V Patterning Defects in *Pbx* Mutant Cortical Progenitors: Altered TF Expression and Increased SMAD1/5 Phosphorylation

It is likely that additional mechanisms contribute to *Pbx1*'s control of cortical region fate, in addition to altered *Emx2* and *Lhx2* expression. Prominent dorsal expansion of *Dbx1* and *Dmrta1* expression (Figure 5) merits further consideration but will require better understanding of the functions of these TFs during cortical development.

PBX proteins function in part through forming complexes with other TALE homeodomains, such as the PKNOX (PREP) and MEIS proteins (Bjerke et al., 2011). *Pbx;Emx1-Cre* mutants have striking overexpression of *Pknox1 (Prep1)* and *Meis2*; both genes have PBX ChIP-seq peaks (Figure 6). It is possible that the increased *Pknox1 (Prep1)* and *Meis2* expression was a compensatory mechanism or that the increase intensifies the phenotype. Future analyses of *Pknox1 (Prep1)* and *Meis2* mutants, alone or in combination with *Pbx1*, are needed to elucidate their respective functions.

As noted earlier, *Pbx;Emx1* mutants had a prominent ventral expansion of dorsal properties in the VZ (*Emx2* and *Lhx2*) (Figure 5) and in the CP (*NT3*) (Figure 2). These mutants also showed increased levels of activated (phosphorylated) pSMAD1/5 TFs (Figures 6J and 6J′). BMP signaling activates SMAD1/5 (Itoh et al., 2000; Kitisin et al., 2007). In the forebrain, BMP signaling is known to specify the choroid plexus, dorsal-most fate in the telencephalon (Fernandes et al., 2007). Thus, it is possible that increased pSMAD1/5 participates in the expansion of dorsal cortical properties in the *Pbx;Emx1* mutant that, in conjunction with the increased *Emx2* and *Lhx2* expression, contributes to the loss of the frontal cortex. We are uncertain about the mechanisms for increased pSMAD1/5 but speculate that loss of *Smoc1* expression (Figures 6H and 6H′) may contribute to this. In *Xenopus* early embryogenesis, there is evidence that *Smoc1* acts as a BMP antagonist (Thomas et al., 2009).

Pbx Function in Newly Born Cortical Neurons Regulates Cortical Patterning

While regional specification of cortical domains is initiated in neuroepithelial stem cells (VZ) by processes that control gene expression, there is evidence, based on loss of *CoupTFI*, *Bhlhb5*, and *Lhx2* functions (Alfano et al., 2014; Joshi et al., 2008; Zembrzycki et al., 2015), that immature CP neurons maintain plasticity regarding cortical regional or areal identity. Here, we found that eliminating *Pbx* function in newly generated cortical neurons using *Nex-Cre* degraded regional cortical molecular properties, particularly in the frontal cortex, which showed greatly reduced *Lmo4* and *NT3* expression (Figure 2).

ChIP-seq analysis identified PBX peaks in the *Lmo3* and *Lmo4* loci, providing evidence that *Pbx* expression in postmitotic neurons (Figure 1) directly regulates these markers of cortical areas. Furthermore, *Lmo4* function is required in rostral cortical neurons to control the identity of its projection neurons (Cederquist et al., 2013). Thus, our data are consistent with the model that *Pbx* expression in cortical progenitors controls region fate through repression of *Emx2* and *Lhx2* and *Pbx* expression in cortical neurons controls their identity by promoting *Lmo4* expression.

Pbx Represses *Reelin* Expression in Rostral CP Neurons: Evidence that Ectopic *Reelin* Expression in *Pbx* Mutants Leads to Dyslamination in the Rostral Cortex

Reelin regulates radial migration of immature cortical projection neurons and orchestrates cortical "inside-out" laminar organization (Ogawa et al., 1995). Here, we found that loss of *Pbx* in cortical progenitors leads to ectopic *Reelin* expression that expands ventrally from indusium griseum (where it is normally present) into the rostral neocortex, particularly in early-born layers (Figure 3). We suggest that abnormal DV patterning in the cortical VZ accounts for much of this ectopic expression. However, loss of *Pbx* in newly generated neurons (*Nex-Cre*) leads to a subtle increase in *Reelin* overexpression (Figure 3), suggesting that *Pbx* regulates Reelin in both the VZ and the cortical neurons.

Consistent with this, there is a prominent PBX ChIP-seq intragenic peak in *Reelin* in both E12.5 and E15.5 analyses (Figure 6I).

The *Pbx;Emx1-Cre* mutant shows a robust lamination phenotype (only in the rostral cortex, where the ectopic *Reelin* is evident) (Figure 4), consistent with the model that ectopic *Reelin* expression disrupts the normal lamination pattern. In the rostral cortex, neurons expressing subplate, layer VI, and layer V markers are in a superficial position, whereas neurons expressing *Cux2*, the layer II/III marker, are in a deep position. BrdU pulse-chase analyses support the inversion of these layers in the rostral cortex (Figure S4). Thus, *Pbx* controls programs that mediate regional and laminar development, particularly in the rostral cortex.

PBX ChIP-Seq from Embryonic Cortex Identifies Target Genes

The anti-PBX antibody used in the ChIP experiments recognizes PBX1, PBX2, and PBX3 (Ferretti et al., 2011). *Pbx3* expression is not detectable in the developing cortex (Allen Brain Atlas). As noted previously, *Pbx1* and *Pbx2* share similar expression during cortical development (Figure 1; Figure S1) and share functions (Capellini et al., 2006, 2008). Thus, the PBX ChIP-seq results most likely reflect both PBX1 and PBX2 genomic binding sites.

We performed PBX ChIP-seq from E12.5 and E15.5 cortex. At E12.5, most cells in the cortex are progenitors; thus, the ~4,100 PBX ChIP-seq peaks from this age should largely reflect PBX-bound regulatory elements in dividing cells of the VZ and SVZ, some of which are generating neurons destined to deep cortical layers. In the E15.5 cortex there are both progenitors and neurons; thus, the ~7,600 PBX ChIP-seq peaks from this age should reflect a mixture of PBX-bound regulatory elements in progenitors and immature neurons. We predict that PBX binding captured by the ChIP-seq experiments includes both activating and repressive activity. In the future, region-specific chromatin datasets across the cortex could be used to examine this at a chromatin level. Nonetheless, we show that PBX binds near genes that are both upregulated and downregulated after conditional deletion of *Pbx1*, evidence for direct PBX regulation of critical patterning genes.

The intersection of the E12.5 and E15.5 ChIP-seq data identified ~1,600 PBX peaks unique to E12.5 data. These may be enriched for regulatory elements that function in cortical progenitors and/or are important in the generation of deep-layer cortical neurons. Conversely, the intersection of the E12.5 and the E15.5 ChIP-seq data showed ~5,100 PBX peaks unique to E15.5. These may be enriched for regulatory elements that function in immature cortical neurons and/or are important in the generation of superficial-layer cortical neurons. Finally, PBX bound to ~2,500 peaks at both E12.5 and E15.5; these regulatory elements may execute functions common to these stages of corticogenesis.

Roughly 20% of PBX ChIP-seq peaks were found close (0–5 kb) to genes, particularly 5′ of the exons, and thus represent, in part, binding to promoters (Figure S6). In addition, >65% of the peaks mapped >5 kb away from transcribed genic regions (Figure S6), suggesting that PBX also binds to enhancers. We identified PBX peaks on 270 regions that have enhancer activity at E11.5 (Table S1); 120 of these regions have enhancer activity in the E11.5 forebrain (Figure S6D; Table S2) (Visel et al., 2013).

Nucleotide Motifs in Genomic Loci Bound by PBX

De novo analysis of motifs from PBX peak sequences identified the likely primary PBX binding motif, which corresponds to a previously described motif for MEIS1 (Knoepfler et al., 1997; Shen et al., 1997). This binding motif occurs as both a full inverted palindromic motif and a set of motifs that are half-sites of the full inverted motif. PBX peaks proximal to TSS were strongly enriched for binding motifs mapped to the SP/EGR family, NRF1, ELK4, MZF1_1-4, and TFAP2A. Thus, PBX proteins may cooperate at promoters with these proteins. The SP family member SP8 has a prominent role in cortical patterning (Borello et al., 2014; Sahara et al., 2007).

Distal PBX peaks were strongly enriched for motifs that are bound by proteins related to PDX1, MECOM/NFATC2, POU5f1::SOX2, FOXP1/SRY, NFATC2, ATOH1, SOX5, and MEF2A. These TFs are likely enhancer regulators, many of which are related to TFs with known functions in cortical development. For instance, the POU5f1::SOX2 complex, which control embryonic stem cell pluripotency, is related to the SOX2 and BRN (POU) proteins that promote neural fate (Tanaka et al., 2004). *Sox5* function is crucial for development of deep-layer neurons (Kwan et al., 2008; Lai et al., 2008; Leone et al., 2008). ATOH1 is a bHLH family member, many of which have fundamental roles in cortical development, including *Ngn1*, *Ngn2*, and the *NeuroD* family (Fode et al., 2000; Mattar et al., 2008; Olson et al., 2001; Sun et al., 2001). The observation that the ATOH1 motif was enriched at E15.5 but not E12.5 (Figures 7C–7F) suggests that PBX and bHLH proteins may coordinately bind to enhancers with activity during neurogenesis, neuronal migration, and maturation rather than in neuroepithelial progenitors. Finally, the FOXP1 motif is consistent with known functions of *FoxP1* and *FoxP2* in neural differentiation (Bacon et al., 2015; Tsui et al., 2013). In sum, these results are an entrée for elucidating the mechanisms whereby combinations of TFs interact with PBX proteins on *cis*-regulatory elements to modulate gene expression during cortical regionalization, laminar patterning, and neuronal differentiation.

EXPERIMENTAL PROCEDURES

ISH on Brain Sections

All experiments were performed according to the University of California San Francisco Institutional Animal Care and Use Committee. The 20 μm frozen sections were dried, washed three times with PBS (5 min each), and fixed with 4% paraformaldehyde in PBS for 10 min. Sections were then rinsed with PBS three times (3 min each) and treated with 1 μg/ml Proteinase K for 17 min. After two quick rinses, PBS sections were postfixed with 4% paraformaldehyde for 5 min and rinsed again in PBS three times (3 min each). Acetylation was performed for 10 min in an acetylation buffer containing 1.3% triethanolamine, 0.17% HCl, and 0.4% acetic anhydride in water. Sections were then rinsed with PBS three times (10 min each) and prehybridized by incubating with hybridization buffer (50% formamide, 5x SSC [pH 4.5], 50 μg/ml yeast tRNA, 1% SDS, 50 μg/ml heparin) for 2 hr in a 67°C oven. After prehybridization, in situ probes diluted in hybridization buffer at 500 ng/ml were added for overnight incubation at 67°C. Next-day slides were rinsed with prewarmed 5x SSC [pH 4.5], washed twice (30 min each) with 0.2x SSC (pH 4.5) at 70°C, and then washed once (5 min) with 0.2x SSC (pH 4.5) at room temperature, followed by a wash with NTT buffer (0.15 M NaCl, 0.1 M Tris [pH 8.0], 0.1% Tween 20).

Sections were blocked with NTT blocking buffer containing 5% heat-inactivated horse serum and 2% blocking buffer (Catalog No. 11096176001, Roche) for 1 hr at room temperature, followed by an overnight incubation at 4°C with anti-digoxigenin-alkaline phosphatase (AP) antibody (1:5,000 dilution in NTT blocking buffer). Next-day sections were washed three times with NTT buffer (30 min each), followed by three 5 min washes with NTTML buffer (0.15 M NaCl, 0.1 M Tris [pH 9.5], 0.1% Tween 20, 50 mM MgCl2, 2 mM levamisole), and incubated with developing reagent BM Purple (Catalog No. 11442074001, Roche) until desired intensity of the signal was reached. Development reaction was stopped with PBS. Sections were allowed to dry, dehydrated with xylenes, and mounted with Permount.

WM-ISH

The meninges were removed from dissected P0 brains, and brains were fixed overnight in 4% paraformaldehyde. After two rinses with PBS containing 0.1% Tween 20 (10 min each), brains were rehydrated through a series of methanol washes in PBS-Tween 20 (25%, 50%, 75%, and 100%) and stored at −20°C until further processing. On the day of the experiment, brains were rehydrated through a series of methanol washes (75%, 50%, and 25%), rinsed with PBS-Tween 20 twice, and treated with 20 μm/ml Proteinase K for 30 min. After digestion, tissue was rinsed with 100 mM glycine and PBS-Tween 20 and postfixed with 4% paraformaldehyde/0.1% glutaraldehyde for 20 min. After postfixation, brains were washed once with PBS-Tween 20 and then washed once with a 1:1 mixture of PBS-Tween 20 and hybridization buffer (50% formamide, 1.3x SSC [pH 4.5], 5 mM EDTA, 50 μg/ml yeast tRNA, 100 μg/ml heparin, 0.5% Tween 20). Solution was then replaced with hybridization buffer, and tissue was allowed to prehybridize for 1 hr at 70°C. In situ probes were diluted in hybridization buffer at 500 ng/ml, and hybridization was performed overnight at 70°C. Next-day brains were washed three times (30 min each, at 70°C) with hybridization buffer, once with a 1:1 mixture of hybridization buffer and Tris-buffered saline and Tween 20 (TBST; 30 min at 70°C) and three times (30 min each) with room-temperature TBST. Brains were blocked with TBST containing 10% heat-inactivated horse serum and 0.1% blocking buffer (Roche) for 2 hr at room temperature, followed by an overnight incubation at 4°C with anti-digoxigenin-AP antibody (1:4,000 dilution). Next-day brains were washed with TBST eight times for 30 min each and left in the wash buffer overnight. BM Purple (Roche) was used as a developing reagent.

Chromatin Immunoprecipitation

Wild-type cortices (one litter of E12.5 or E15.5) were dissected, triturated in 1% formaldehyde in PBS, and fixed for a total of 10 min at room temperature. Fixed cells were pelleted and washed with cold PBS. Pellets were lysed in 500 μl of lysis buffer (1% SDS, 10 mM EDTA, 50 mM Tris [pH 8.1]) on ice for 10 min, and lysates were sonicated using Bioruptor (Diagenode) on high settings for 15 cycles (7.5 min of total sonication time). The resulting average chromatin size was 200–500 bp as verified by the bioanalyzer. Cleared chromatin was diluted ten times with dilution buffer (0.01% SDS, 1.1% Triton X-100, 1.2 mM EDTA, 16.7 mM Tris-HCl [pH 8.1], 167 mM NaCl) and was incubated overnight at 4°C with 3 μg of appropriate antibody. Mixture of protein A and G magnetic beads (Life Technologies) was preblocked overnight with BSA and tRNA and was added to the chromatin the next day for 3 hr. Immune complexes were washed once with low-salt buffer (0.1% SDS, 1% Triton X-100, 2 mM EDTA, 20 mM Tris-HCl [pH 8.1], 150 mM NaCl), high-salt buffer (0.1% SDS, 1% Triton X-100, 2 mM EDTA, 20 mM Tris-HCl [pH 8.1], 500 mM NaCl), LiCl buffer (0.25 M LiCl, 1% Tergitol-type nonyl phenoxypolyethoxylethanol 40, 1% deoxycholic acid [sodium salt], 1 mM EDTA, 10 mM Tris [pH 8.1]), and Tris-EDTA buffer. Complexes were eluted in 1% SDS, 10 mM sodium bicarbonate buffer at 65°C for 10 min. Crosslinks were reversed at 65°C overnight, proteins were digested using proteinase K, and DNA was purified using the Zymo ChIP DNA Clean and Concentrator kit (Zymo Research). Immunoprecipitation was performed using the following antibody: Pbx1/2/3 (sc-888, Santa Cruz). As a negative control in PBX ChIP experiments, the PBX antibody was incubated with PBX blocking peptide (sc-888P, Santa Cruz) at a 1:400 molar ratio and added to the chromatin lysates. ChIP-seq libraries were prepared using the NEBNext DNA Library Prep Kit (NEB) and Illumina standard adaptors and were sequenced using a 50 bp single-end strategy using Illumina HiSeq platform.

ACCESSION NUMBERS

The accession number for the data reported in this paper is GEO: GSE73288.

SUPPLEMENTAL INFORMATION

Supplemental Information includes Supplemental Experimental Procedures, seven figures, and two tables and can be found with this article online at http://dx.doi.org/10.1016/j.neuron.2015.10.045.

AUTHOR CONTRIBUTIONS

O.G. designed, conducted, and analyzed data for all experiments described in this manuscript. S.L. helped perform and analyze ChIP-seq experiments and provided comments on the manuscript. A.N., P.L.F.T., and A.V. performed informatic analyses of the ChIP-seq data. A.R.Y. performed analysis of *Pbx2* mutants. L.S. and E.F. provided the *Pbx* mutant mice and information about the PBX antibodies. J.L.R.R. provided funding and laboratory resources and helped guide the project and analyze results. O.G. and J.L.R.R. prepared the manuscript.

ACKNOWLEDGMENTS

This work was supported by funds from NARSAD to O.G., and Nina Ireland, Weston Havens Foundation, NINDS (NS34661), and NIMH (MH049428 and MH081880) to J.L.R.R. A.V. was supported by NIH grants R01HG003988 and U54HG006997. Research conducted at the E.O. Lawrence Berkeley National Laboratory was performed under Department of Energy Contract DE-AC02-05CH11231, University of California. J.L.R.R. is a founder and consultant for *Neurona*; this company has no financial interests related to this paper.

Received: March 24, 2015
Revised: August 13, 2015
Accepted: October 13, 2015
Published: December 3, 2015

REFERENCES

Alfano, C., Magrinelli, E., Harb, K., Hevner, R.F., and Studer, M. (2014). Postmitotic control of sensory area specification during neocortical development. Nat. Commun. *5*, 5632.

Amaral, D.G., Schumann, C.M., and Nordahl, C.W. (2008). Neuroanatomy of autism. Trends Neurosci. *31*, 137–145.

Armentano, M., Chou, S.J., Tomassy, G.S., Leingärtner, A., O'Leary, D.D., and Studer, M. (2007). COUP-TFI regulates the balance of cortical patterning between frontal/motor and sensory areas. Nat. Neurosci. *10*, 1277–1286.

Bacon, C., Schneider, M., Le Magueresse, C., Froehlich, H., Sticht, C., Gluch, C., Monyer, H., and Rappold, G.A. (2015). Brain-specific Foxp1 deletion impairs neuronal development and causes autistic-like behaviour. Mol. Psychiatry *20*, 632–639.

Bedogni, F., Hodge, R.D., Elsen, G.E., Nelson, B.R., Daza, R.A., Beyer, R.P., Bammler, T.K., Rubenstein, J.L., and Hevner, R.F. (2010). Tbr1 regulates regional and laminar identity of postmitotic neurons in developing neocortex. Proc. Natl. Acad. Sci. USA *107*, 13129–13134.

Berthelsen, J., Viggiano, L., Schulz, H., Ferretti, E., Consalez, G.G., Rocchi, M., and Blasi, F. (1998a). PKNOX1, a gene encoding PREP1, a new regulator of Pbx activity, maps on human chromosome 21q22.3 and murine chromosome 17B/C. Genomics *47*, 323–324.

Berthelsen, J., Zappavigna, V., Ferretti, E., Mavilio, F., and Blasi, F. (1998b). The novel homeoprotein Prep1 modulates Pbx-Hox protein cooperativity. EMBO J. *17*, 1434–1445.

Berthelsen, J., Zappavigna, V., Mavilio, F., and Blasi, F. (1998c). Prep1, a novel functional partner of Pbx proteins. EMBO J. *17*, 1423–1433.

Bishop, K.M., Goudreau, G., and O'Leary, D.D. (2000). Regulation of area identity in the mammalian neocortex by Emx2 and Pax6. Science *288*, 344–349.

Bjerke, G.A., Hyman-Walsh, C., and Wotton, D. (2011). Cooperative transcriptional activation by Klf4, Meis2, and Pbx1. Mol. Cell. Biol. *31*, 3723–3733.

Borello, U., Madhavan, M., Vilinsky, I., Faedo, A., Pierani, A., Rubenstein, J., and Campbell, K. (2014). Sp8 and COUP-TF1 reciprocally regulate patterning and Fgf signaling in cortical progenitors. Cereb. Cortex *24*, 1409–1421.

Bulchand, S., Grove, E.A., Porter, F.D., and Tole, S. (2001). LIM-homeodomain gene Lhx2 regulates the formation of the cortical hem. Mech. Dev. *100*, 165–175.

Bürglin, T.R. (1997). Analysis of TALE superclass homeobox genes (MEIS, PBC, KNOX, Iroquois, TGIF) reveals a novel domain conserved between plants and animals. Nucleic Acids Res. *25*, 4173–4180.

Capellini, T.D., Di Giacomo, G., Salsi, V., Brendolan, A., Ferretti, E., Srivastava, D., Zappavigna, V., and Selleri, L. (2006). Pbx1/Pbx2 requirement for distal limb patterning is mediated by the hierarchical control of Hox gene spatial distribution and Shh expression. Development *133*, 2263–2273.

Capellini, T.D., Zewdu, R., Di Giacomo, G., Asciutti, S., Kugler, J.E., Di Gregorio, A., and Selleri, L. (2008). Pbx1/Pbx2 govern axial skeletal development by controlling Polycomb and Hox in mesoderm and Pax1/Pax9 in sclerotome. Dev. Biol. *321*, 500–514.

Capellini, T.D., Handschuh, K., Quintana, L., Ferretti, E., Di Giacomo, G., Fantini, S., Vaccari, G., Clarke, S.L., Wenger, A.M., Bejerano, G., et al. (2011a). Control of pelvic girdle development by genes of the Pbx family and Emx2. Dev. Dyn. *240*, 1173–1189.

Capellini, T.D., Zappavigna, V., and Selleri, L. (2011b). Pbx homeodomain proteins: TALEnted regulators of limb patterning and outgrowth. Dev. Dyn. *240*, 1063–1086.

Caronia-Brown, G., Yoshida, M., Gulden, F., Assimacopoulos, S., and Grove, E.A. (2014). The cortical hem regulates the size and patterning of neocortex. Development *141*, 2855–2865.

Cederquist, G.Y., Azim, E., Shnider, S.J., Padmanabhan, H., and Macklis, J.D. (2013). Lmo4 establishes rostral motor cortex projection neuron subtype diversity. J. Neurosci. *33*, 6321–6332.

Cholfin, J.A., and Rubenstein, J.L. (2007). Patterning of frontal cortex subdivisions by Fgf17. Proc. Natl. Acad. Sci. USA *104*, 7652–7657.

Cholfin, J.A., and Rubenstein, J.L. (2008). Frontal cortex subdivision patterning is coordinately regulated by Fgf8, Fgf17, and Emx2. J. Comp. Neurol. *509*, 144–155.

Chou, S.J., Perez-Garcia, C.G., Kroll, T.T., and O'Leary, D.D. (2009). Lhx2 specifies regional fate in Emx1 lineage of telencephalic progenitors generating cerebral cortex. Nat. Neurosci. *12*, 1381–1389.

Chou, S.J., Babot, Z., Leingärtner, A., Studer, M., Nakagawa, Y., and O'Leary, D.D. (2013). Geniculocortical input drives genetic distinctions between primary and higher-order visual areas. Science *340*, 1239–1242.

Crespo-Facorro, B., Kim, J., Andreasen, N.C., O'Leary, D.S., Bockholt, H.J., and Magnotta, V. (2000). Insular cortex abnormalities in schizophrenia: a structural magnetic resonance imaging study of first-episode patients. Schizophr. Res. *46*, 35–43.

DiMartino, J.F., Selleri, L., Traver, D., Firpo, M.T., Rhee, J., Warnke, R., O'Gorman, S., Weissman, I.L., and Cleary, M.L. (2001). The Hox cofactor and proto-oncogene Pbx1 is required for maintenance of definitive hematopoiesis in the fetal liver. Blood *98*, 618–626.

Elsen, G.E., Hodge, R.D., Bedogni, F., Daza, R.A., Nelson, B.R., Shiba, N., Reiner, S.L., and Hevner, R.F. (2013). The protomap is propagated to cortical plate neurons through an Eomes-dependent intermediate map. Proc. Natl. Acad. Sci. USA *110*, 4081–4086.

Faedo, A., Tomassy, G.S., Ruan, Y., Teichmann, H., Krauss, S., Pleasure, S.J., Tsai, S.Y., Tsai, M.J., Studer, M., and Rubenstein, J.L. (2008). COUP-TFI coordinates cortical patterning, neurogenesis, and laminar fate and modulates MAPK/ERK, AKT, and beta-catenin signaling. Cereb. Cortex *18*, 2117–2131.

Fernandes, M., Gutin, G., Alcorn, H., McConnell, S.K., and Hébert, J.M. (2007). Mutations in the BMP pathway in mice support the existence of two molecular classes of holoprosencephaly. Development *134*, 3789–3794.

Ferretti, E., Li, B., Zewdu, R., Wells, V., Hebert, J.M., Karner, C., Anderson, M.J., Williams, T., Dixon, J., Dixon, M.J., et al. (2011). A conserved Pbx-Wnt-p63-Irf6 regulatory module controls face morphogenesis by promoting epithelial apoptosis. Dev. Cell *21*, 627–641.

Ficara, F., Murphy, M.J., Lin, M., and Cleary, M.L. (2008). Pbx1 regulates self-renewal of long-term hematopoietic stem cells by maintaining their quiescence. Cell Stem Cell *2*, 484–496.

Fode, C., Ma, Q., Casarosa, S., Ang, S.L., Anderson, D.J., and Guillemot, F. (2000). A role for neural determination genes in specifying the dorsoventral identity of telencephalic neurons. Genes Dev. *14*, 67–80.

Fukuchi-Shimogori, T., and Grove, E.A. (2001). Neocortex patterning by the secreted signaling molecule FGF8. Science *294*, 1071–1074.

Galceran, J., Miyashita-Lin, E.M., Devaney, E., Rubenstein, J.L., and Grosschedl, R. (2000). Hippocampus development and generation of dentate gyrus granule cells is regulated by LEF1. Development *127*, 469–482.

Garel, S., Huffman, K.J., and Rubenstein, J.L. (2003). Molecular regionalization of the neocortex is disrupted in Fgf8 hypomorphic mutants. Development *130*, 1903–1914.

Goebbels, S., Bormuth, I., Bode, U., Hermanson, O., Schwab, M.H., and Nave, K.A. (2006). Genetic targeting of principal neurons in neocortex and hippocampus of NEX-Cre mice. Genesis *44*, 611–621.

Gorski, J.A., Talley, T., Qiu, M., Puelles, L., Rubenstein, J.L., and Jones, K.R. (2002). Cortical excitatory neurons and glia, but not GABAergic neurons, are produced in the Emx1-expressing lineage. J. Neurosci. *22*, 6309–6314.

Goumans, M.J., and Mummery, C. (2000). Functional analysis of the TGFbeta receptor/Smad pathway through gene ablation in mice. Int. J. Dev. Biol. *44*, 253–265.

Gourion, D., Gourevitch, R., Leprovost, J.B., Olié H lôo, J.P., and Krebs, M.O. (2004). Neurodevelopmental hypothesis in schizophrenia. Encephale *30*, 109–118.

Greig, L.C., Woodworth, M.B., Galazo, M.J., Padmanabhan, H., and Macklis, J.D. (2013). Molecular logic of neocortical projection neuron specification, development and diversity. Nat. Rev. Neurosci. *14*, 755–769.

Hamasaki, T., Leingärtner, A., Ringstedt, T., and O'Leary, D.D. (2004). EMX2 regulates sizes and positioning of the primary sensory and motor areas in neocortex by direct specification of cortical progenitors. Neuron *43*, 359–372.

Hoerder-Suabedissen, A., Wang, W.Z., Lee, S., Davies, K.E., Goffinet, A.M., Rakić, S., Parnavelas, J., Reim, K., Nicolić, M., Paulsen, O., and Molnár, Z. (2009). Novel markers reveal subpopulations of subplate neurons in the murine cerebral cortex. Cereb. Cortex *19*, 1738–1750.

Itoh, S., Itoh, F., Goumans, M.J., and Ten Dijke, P. (2000). Signaling of transforming growth factor-beta family members through Smad proteins. Eur. J. Biochem. *267*, 6954–6967.

Joshi, P.S., Molyneaux, B.J., Feng, L., Xie, X., Macklis, J.D., and Gan, L. (2008). Bhlhb5 regulates the postmitotic acquisition of area identities in layers II–V of the developing neocortex. Neuron *60*, 258–272.

Kikkawa, T., Obayashi, T., Takahashi, M., Fukuzaki-Dohi, U., Numayama-Tsuruta, K., and Osumi, N. (2013). Dmrta1 regulates proneural gene expression downstream of Pax6 in the mammalian telencephalon. Genes Cells *18*, 636–649.

Kitisin, K., Saha, T., Blake, T., Golestaneh, N., Deng, M., Kim, C., Tang, Y., Shetty, K., Mishra, B., and Mishra, L. (2007). Tgf-beta signaling in development. Sci. STKE *2007*, cm1.

Knoepfler, P.S., Calvo, K.R., Chen, H., Antonarakis, S.E., and Kamps, M.P. (1997). Meis1 and pKnox1 bind DNA cooperatively with Pbx1 utilizing an interaction surface disrupted in oncoprotein E2a-Pbx1. Proc. Natl. Acad. Sci. USA *94*, 14553–14558.

Konno, D., Iwashita, M., Satoh, Y., Momiyama, A., Abe, T., Kiyonari, H., and Matsuzaki, F. (2012). The mammalian DM domain transcription factor

Dmrta2 is required for early embryonic development of the cerebral cortex. PLoS ONE *7*, e46577.

Koss, M., Bolze, A., Brendolan, A., Saggese, M., Capellini, T.D., Bojilova, E., Boisson, B., Prall, O.W., Elliott, D.A., Solloway, M., et al. (2012). Congenital asplenia in mice and humans with mutations in a Pbx/Nkx2-5/p15 module. Dev. Cell *22*, 913–926.

Kwan, K.Y., Lam, M.M., Krsnik, Z., Kawasawa, Y.I., Lefebvre, V., and Sestan, N. (2008). SOX5 postmitotically regulates migration, postmigratory differentiation, and projections of subplate and deep-layer neocortical neurons. Proc. Natl. Acad. Sci. USA *105*, 16021–16026.

Lai, T., Jabaudon, D., Molyneaux, B.J., Azim, E., Arlotta, P., Menezes, J.R., and Macklis, J.D. (2008). SOX5 controls the sequential generation of distinct corticofugal neuron subtypes. Neuron *57*, 232–247.

Lee, S.M., Tole, S., Grove, E., and McMahon, A.P. (2000). A local Wnt-3a signal is required for development of the mammalian hippocampus. Development *127*, 457–467.

Leone, D.P., Srinivasan, K., Chen, B., Alcamo, E., and McConnell, S.K. (2008). The determination of projection neuron identity in the developing cerebral cortex. Curr. Opin. Neurobiol. *18*, 28–35.

Li, G., Adesnik, H., Li, J., Long, J., Nicoll, R.A., Rubenstein, J.L., and Pleasure, S.J. (2008). Regional distribution of cortical interneurons and development of inhibitory tone are regulated by Cxcl12/Cxcr4 signaling. J. Neurosci. *28*, 1085–1098.

Long, J.E., Swan, C., Liang, W.S., Cobos, I., Potter, G.B., and Rubenstein, J.L. (2009). Dlx1&2 and Mash1 transcription factors control striatal patterning and differentiation through parallel and overlapping pathways. J. Comp. Neurol. *512*, 556–572.

Mallamaci, A., and Stoykova, A. (2006). Gene networks controlling early cerebral cortex arealization. Eur. J. Neurosci. *23*, 847–856.

Mallamaci, A., Muzio, L., Chan, C.H., Parnavelas, J., and Boncinelli, E. (2000). Area identity shifts in the early cerebral cortex of *Emx2*$^{-/-}$ mutant mice. Nat. Neurosci. *3*, 679–686.

Mangale, V.S., Hirokawa, K.E., Satyaki, P.R., Gokulchandran, N., Chikbire, S., Subramanian, L., Shetty, A.S., Martynoga, B., Paul, J., Mai, M.V., et al. (2008). Lhx2 selector activity specifies cortical identity and suppresses hippocampal organizer fate. Science *319*, 304–309.

Mattar, P., Langevin, L.M., Markham, K., Klenin, N., Shivji, S., Zinyk, D., and Schuurmans, C. (2008). Basic helix-loop-helix transcription factors cooperate to specify a cortical projection neuron identity. Mol. Cell. Biol. *28*, 1456–1469.

McCloy, R.A., Rogers, S., Caldon, C.E., Lorca, T., Castro, A., and Burgess, A. (2014). Partial inhibition of Cdk1 in G 2 phase overrides the SAC and decouples mitotic events. Cell Cycle *13*, 1400–1412.

McLean, C.Y., Bristor, D., Hiller, M., Clarke, S.L., Schaar, B.T., Lowe, C.B., Wenger, A.M., and Bejerano, G. (2010). GREAT improves functional interpretation of *cis*-regulatory regions. Nat. Biotechnol. *28*, 495–501.

Miyashita-Lin, E.M., Hevner, R., Wassarman, K.M., Martinez, S., and Rubenstein, J.L. (1999). Early neocortical regionalization in the absence of thalamic innervation. Science *285*, 906–909.

Molyneaux, B.J., Arlotta, P., Menezes, J.R., and Macklis, J.D. (2007). Neuronal subtype specification in the cerebral cortex. Nat. Rev. Neurosci. *8*, 427–437.

Monuki, E.S., Porter, F.D., and Walsh, C.A. (2001). Patterning of the dorsal telencephalon and cerebral cortex by a roof plate-Lhx2 pathway. Neuron *32*, 591–604.

Muzio, L., and Mallamaci, A. (2003). Emx1, emx2 and pax6 in specification, regionalization and arealization of the cerebral cortex. Cereb. Cortex *13*, 641–647.

Nakagawa, Y., Johnson, J.E., and O'Leary, D.D. (1999). Graded and areal expression patterns of regulatory genes and cadherins in embryonic neocortex independent of thalamocortical input. J. Neurosci. *19*, 10877–10885.

Nieto, M., Monuki, E.S., Tang, H., Imitola, J., Haubst, N., Khoury, S.J., Cunningham, J., Gotz, M., and Walsh, C.A. (2004). Expression of Cux-1 and Cux-2 in the subventricular zone and upper layers II–IV of the cerebral cortex. J. Comp. Neurol. *479*, 168–180.

Ogawa, M., Miyata, T., Nakajima, K., Yagyu, K., Seike, M., Ikenaka, K., Yamamoto, H., and Mikoshiba, K. (1995). The reeler gene-associated antigen on Cajal-Retzius neurons is a crucial molecule for laminar organization of cortical neurons. Neuron *14*, 899–912.

Olson, J.M., Asakura, A., Snider, L., Hawkes, R., Strand, A., Stoeck, J., Hallahan, A., Pritchard, J., and Tapscott, S.J. (2001). NeuroD2 is necessary for development and survival of central nervous system neurons. Dev. Biol. *234*, 174–187.

Phelan, M.L., Rambaldi, I., and Featherstone, M.S. (1995). Cooperative interactions between HOX and PBX proteins mediated by a conserved peptide motif. Mol. Cell. Biol. *15*, 3989–3997.

Pierani, A., Moran-Rivard, L., Sunshine, M.J., Littman, D.R., Goulding, M., and Jessell, T.M. (2001). Control of interneuron fate in the developing spinal cord by the progenitor homeodomain protein Dbx1. Neuron *29*, 367–384.

Piven, J., Arndt, S., Bailey, J., Havercamp, S., Andreasen, N.C., and Palmer, P. (1995). An MRI study of brain size in autism. Am. J. Psychiatry *152*, 1145–1149.

Sahara, S., Kawakami, Y., Izpisua Belmonte, J.C., and O'Leary, D.D. (2007). Sp8 exhibits reciprocal induction with Fgf8 but has an opposing effect on anterior-posterior cortical area patterning. Neural Dev. *2*, 10.

Schaeren-Wiemers, N., André, E., Kapfhammer, J.P., and Becker-André, M. (1997). The expression pattern of the orphan nuclear receptor RORbeta in the developing and adult rat nervous system suggests a role in the processing of sensory information and in circadian rhythm. Eur. J. Neurosci. *9*, 2687–2701.

Selleri, L., Depew, M.J., Jacobs, Y., Chanda, S.K., Tsang, K.Y., Cheah, K.S., Rubenstein, J.L., O'Gorman, S., and Cleary, M.L. (2001). Requirement for Pbx1 in skeletal patterning and programming chondrocyte proliferation and differentiation. Development *128*, 3543–3557.

Selleri, L., DiMartino, J., van Deursen, J., Brendolan, A., Sanyal, M., Boon, E., Capellini, T., Smith, K.S., Rhee, J., Pöpperl, H., et al. (2004). The TALE homeodomain protein Pbx2 is not essential for development and long-term survival. Mol. Cell. Biol. *24*, 5324–5331.

Shen, W.F., Chang, C.P., Rozenfeld, S., Sauvageau, G., Humphries, R.K., Lu, M., Lawrence, H.J., Cleary, M.L., and Largman, C. (1996). Hox homeodomain proteins exhibit selective complex stabilities with Pbx and DNA. Nucleic Acids Res. *24*, 898–906.

Shen, W.F., Montgomery, J.C., Rozenfeld, S., Moskow, J.J., Lawrence, H.J., Buchberg, A.M., and Largman, C. (1997). AbdB-like Hox proteins stabilize DNA binding by the Meis1 homeodomain proteins. Mol. Cell. Biol. *17*, 6448–6458.

Stoykova, A., Treichel, D., Hallonet, M., and Gruss, P. (2000). Pax6 modulates the dorsoventral patterning of the mammalian telencephalon. J. Neurosci. *20*, 8042–8050.

Sun, Y., Nadal-Vicens, M., Misono, S., Lin, M.Z., Zubiaga, A., Hua, X., Fan, G., and Greenberg, M.E. (2001). Neurogenin promotes neurogenesis and inhibits glial differentiation by independent mechanisms. Cell *104*, 365–376.

Suzuki, R., and Shimodaira, H. (2006). Pvclust: an R package for assessing the uncertainty in hierarchical clustering. Bioinformatics *22*, 1540–1542.

Swift, G.H., Liu, Y., Rose, S.D., Bischof, L.J., Steelman, S., Buchberg, A.M., Wright, C.V., and MacDonald, R.J. (1998). An endocrine-exocrine switch in the activity of the pancreatic homeodomain protein PDX1 through formation of a trimeric complex with PBX1b and MRG1 (MEIS2). Mol. Cell. Biol. *18*, 5109–5120.

Tanaka, S., Kamachi, Y., Tanouchi, A., Hamada, H., Jing, N., and Kondoh, H. (2004). Interplay of SOX and POU factors in regulation of the Nestin gene in neural primordial cells. Mol. Cell. Biol. *24*, 8834–8846.

Thomas, J.T., Canelos, P., Luyten, F.P., and Moos, M., Jr. (2009). *Xenopus* SMOC-1 inhibits bone morphogenetic protein signaling downstream of receptor binding and is essential for postgastrulation development in *Xenopus*. J. Biol. Chem. *284*, 18994–19005.

Thomas-Chollier, M., Herrmann, C., Defrance, M., Sand, O., Thieffry, D., and van Helden, J. (2012). RSAT peak-motifs: motif analysis in full-size ChIP-seq datasets. Nucleic Acids Res. *40*, e31.

Toresson, H., Parmar, M., and Campbell, K. (2000). Expression of Meis and Pbx genes and their protein products in the developing telencephalon: implications for regional differentiation. Mech. Dev. *94*, 183–187.

Tsui, D., Vessey, J.P., Tomita, H., Kaplan, D.R., and Miller, F.D. (2013). FoxP2 regulates neurogenesis during embryonic cortical development. J. Neurosci. *33*, 244–258.

Visel, A., Blow, M.J., Li, Z., Zhang, T., Akiyama, J.A., Holt, A., Plajzer-Frick, I., Shoukry, M., Wright, C., Chen, F., et al. (2009). ChIP-seq accurately predicts tissue-specific activity of enhancers. Nature *457*, 854–858.

Visel, A., Taher, L., Girgis, H., May, D., Golonzhka, O., Hoch, R.V., McKinsey, G.L., Pattabiraman, K., Silberberg, S.N., Blow, M.J., et al. (2013). A high-resolution enhancer atlas of the developing telencephalon. Cell *152*, 895–908.

Vitobello, A., Ferretti, E., Lampe, X., Vilain, N., Ducret, S., Ori, M., Spetz, J.F., Selleri, L., and Rijli, F.M. (2011). Hox and Pbx factors control retinoic acid synthesis during hindbrain segmentation. Dev. Cell *20*, 469–482.

Wang, Y., Li, G., Stanco, A., Long, J.E., Crawford, D., Potter, G.B., Pleasure, S.J., Behrens, T., and Rubenstein, J.L. (2011). CXCR4 and CXCR7 have distinct functions in regulating interneuron migration. Neuron *69*, 61–76.

Yamasue, H., Iwanami, A., Hirayasu, Y., Yamada, H., Abe, O., Kuroki, N., Fukuda, R., Tsujii, K., Aoki, S., Ohtomo, K., et al. (2004). Localized volume reduction in prefrontal, temporolimbic, and paralimbic regions in schizophrenia: an MRI parcellation study. Psychiatry Res. *131*, 195–207.

Yun, K., Potter, S., and Rubenstein, J.L. (2001). Gsh2 and Pax6 play complementary roles in dorsoventral patterning of the mammalian telencephalon. Development *128*, 193–205.

Zembrzycki, A., Perez-Garcia, C.G., Wang, C.F., Chou, S.J., and O'Leary, D.D. (2015). Postmitotic regulation of sensory area patterning in the mammalian neocortex by Lhx2. Proc. Natl. Acad. Sci. USA *112*, 6736–6741.

Zhou, C.J., Borello, U., Rubenstein, J.L., and Pleasure, S.J. (2006). Neuronal production and precursor proliferation defects in the neocortex of mice with loss of function in the canonical Wnt signaling pathway. Neuroscience *142*, 1119–1131.